CHAPTER 3

Results and discussion

The adsorption behavior of Cd(II) and Zn(II) in single and binary component systems was investigated using leonardite as adsorbent. In this research, the characteristics and properties of leonardite were first determined. Different techniques were used for the characterization of leonardite including XRF, XRD, FTIR, and SEM. The properties of leonardite such as particle size, surface area, pH, cation exchange capacity, and density were also determined. Acknowledgement of the adsorbent properties enlightens on the adsorption behavior. The next step was the adsorption study. The parameters that affects the adsorption including pH value, contact time, metal concentration, and temperature were investigated. The adsorption kinetics, isotherms and thermodynamics were also studied. The last part was the adsorption of Cd(II) and Zn(II) ions in the binary component systems. The isotherm parameters and evaluation of adsorption isotherm model were performed using the linear regression and the non-linear regression. The method of normalization was also applied for the selection of isotherm parameters. The results of such investigation are about to be discussed in the following sections.

3.1 Characteristic and properties of leonardite

3.1.1) Chemical compositions

The chemical compositions of leonardite, determined by the X-ray fluorescence technique (XRF) are given in Table 3.1. It shows the presence of alumina (Al_2O_3), silica (SiO_2), and ferric oxide (Fe_2O_3) as the major inorganic component in leonardite whereas the other oxides are presented in trace amount (< 3%wt). Leonardite composed of alumina 16.28%, silica 28.95%, and ferric oxide 10.37%. The loss on ignition indicated that leonardite contained less than 36.80% organic matter.

Table 3.1 Chemical compositions of leonardite

Chemical composition	%wt
Al_2O_3	16.28
SiO_2	28.95
MgO	0.84
P_2O_5	0.68
K_2O	2.29
CaO	2.83
TiO_2	0.73
Fe_2O_3	10.37
SrO	0.11
ZrO_2	0.086
LOI and etc.	36.87

3.1.2) Mineral compositions

Mineralogical compositions of leonardite, observed by X-ray diffraction technique (XRD) are shown in Fig. 3.1. The result shows that leonardite composed of 3 types of minerals including:

- quartz (SiO_2)
- illite ($(K,H_3O)(Al,Mg,Fe)_2(Si,Al)_4O_{10}[(OH)_2,(H_2O)]$)
- muscovite ($KAl_2(AlSi_3O_{10})(F,OH)_2$, or $(KF)_2(Al_2O_3)_3(SiO_2)_6(H_2O)$)

It can be seen that the elements containing in quartz, illite, and muscovite corresponded well to the results from XRF analysis.

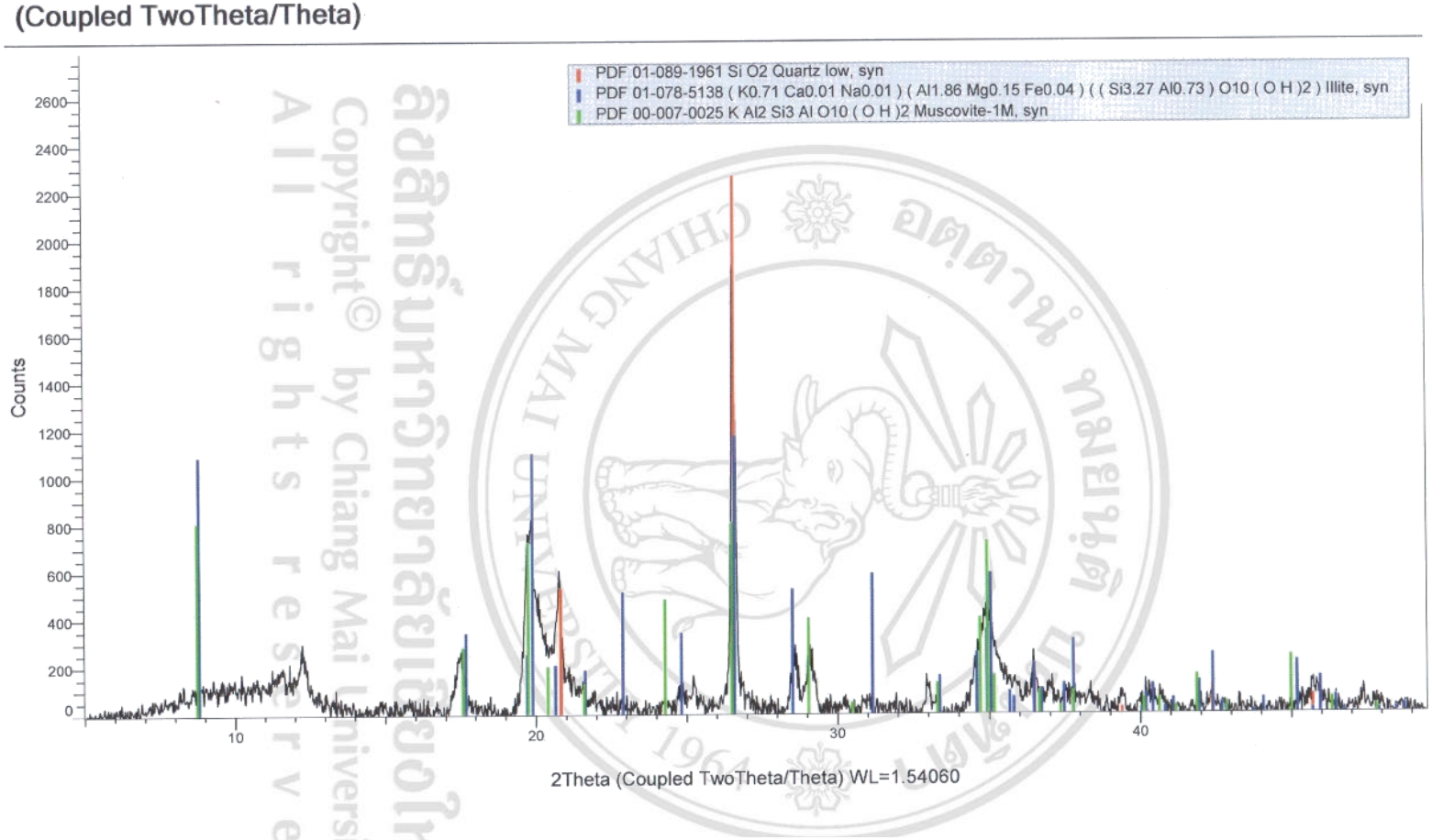

Fig. 3.1 XRD pattern of leonardite

3.1.3) Characterization by FTIR

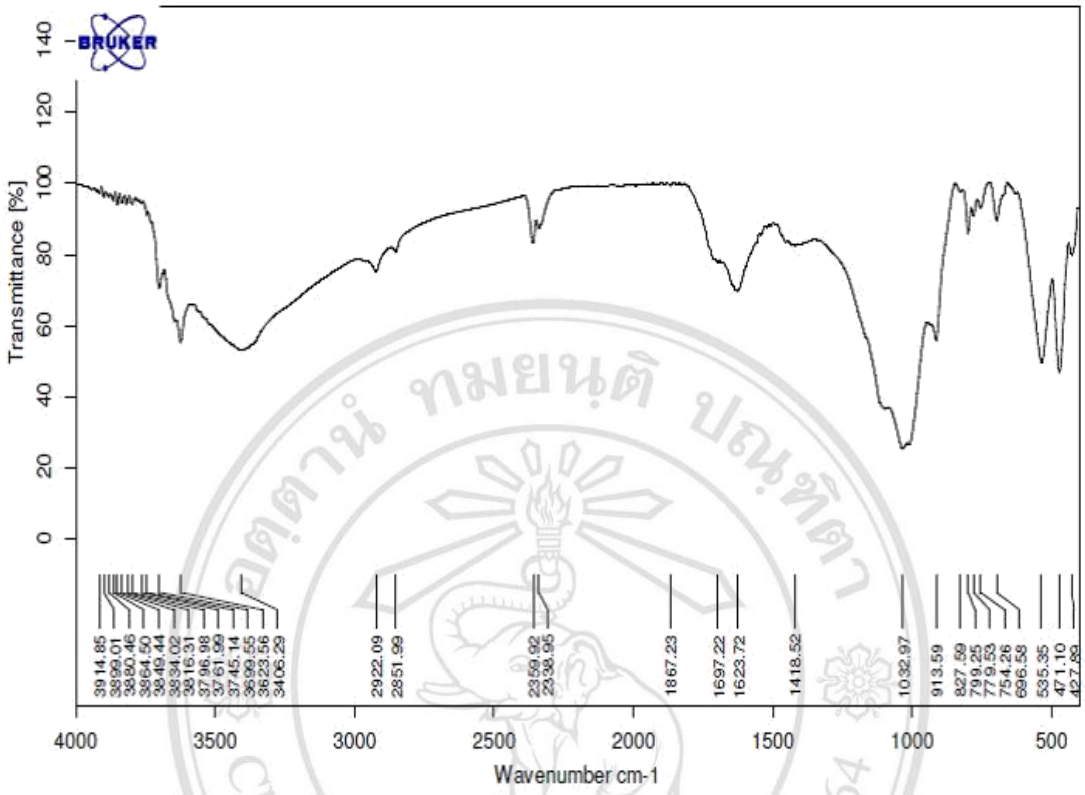

Fig. 3.2 FTIR spectrum of leonardite

The FTIR spectrum is helpful in the identification of sample and also gives the information about functional groups presenting in the sample. Upon consideration of the FTIR spectrum of leonardite in Fig. 3.2, the absorption bands of both inorganic and organic matters are revealed. For the inorganic matter, most of the absorption bands assigned to clay minerals are observed in the region of 3800 – 3200 cm^{-1} and below 1250 cm^{-1}. The stretching vibration of the Si–O groups at 1033, 799, and 780 cm^{-1} with the bending vibration of Si-O groups at 697, 535, and 471 cm^{-1} are assigned to quartz [77-78]. The stretching vibration of O-H groups at 3406 cm^{-1}, the Al-OH-Mg deformation at 827 cm^{-1}, the Al-O-Si vibration at 754 cm^{-1} and Al-OH-Al deformation at 914 cm^{-1} indicated illite. It was considerably difficult to identify the difference between illite and muscovite because both minerals exhibited similar absorption bands [79]. The result obtained from FTIR confirmed the presence of quartz, illite, and muscovite in leonardite.

The FTIR spectrum of leonardite also revealed the absorption bands of organic matter "humic acid" as reported by the literatures [80-81]. The comparison of absorption bands between humic acid and leonardite is shown in Table 3.2. The broad band between 3600 - 3200 cm^{-1} is assigned to the O-H/N-H stretching vibration of phenols, amines/amides, and carboxylic acids. The double bands at 2922 and 2852 cm^{-1} attributed to C-H stretching vibration of alkanes. The stretching vibration band of C=O groups of carboxylic acids and ketones is observed around 1698 cm^{-1}. The presence of absorption band at 1629 cm^{-1} was due to stretching vibration of C=C bonds in aromatic rings and possibly to the stretching vibration of C=O of conjugated ketones and carboxylic groups. The absorption band at 1419 cm^{-1} is assigned to C-H bending vibration of alkanes. The absorption bands of leonardite were in agreement with the data of humic acid.

Table 3.2 The comparison of absorption bands between humic acid and leonardite

Absorption band (cm^{-1})		
Humic acid [80-81]	Leonardite (This work)	Assignment
3399	3406	O-H/N-H stretching vibration
2921, 2852	2922, 2852	C-H stretching vibration
1718	1698	C=O stretching vibration
1618	1629	C=C stretching vibration C=O stretching vibration
1420	1419	C-H bending vibration

3.1.4) Morphology

Leonardite microstructure was determined by SEM (Fig. 3.3). It showed that leonardite has a discontinuous structure with the presence of individual plates.

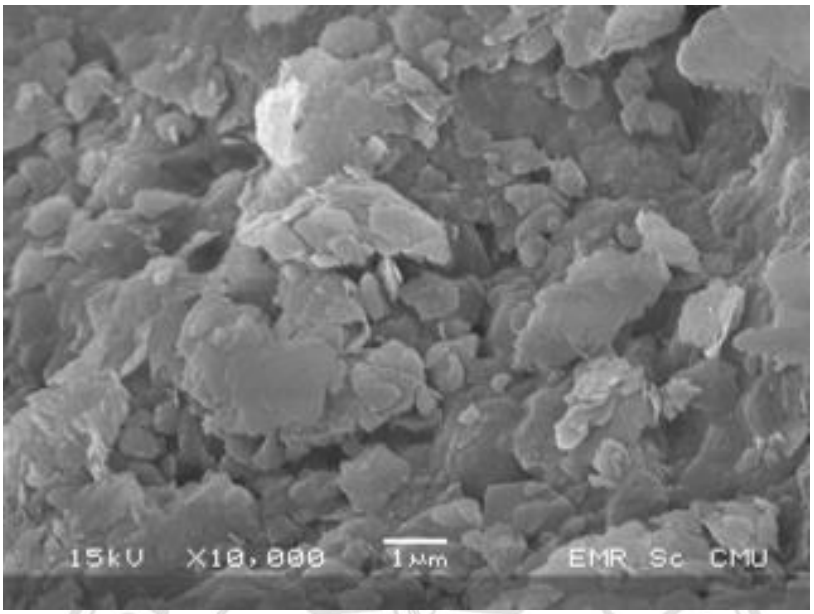

Fig. 3.3 SEM image of leonardite

3.1.5) Properties of leonardite

The particle size distribution, average surface area, pH, cation exchange capacity and density of leonardite are summarized in Table 3.3. It was observed that the pH of leonardite was quite low which expressed the strongly acidity of leonardite. The cation exchange capacity of leonardite was considerably high. This indicated the good ability of leonardite for holding the exchangeable cations.

Table 3.3 Properties of leonardite

Property	content
Particle size (μm)	32.97
Surface area (m^2/g)	19.67
pH	2.40
Cation exchange capacity (cmol/kg)	60.11
Density (g/cm^3)	1.90

3.2 Single-component adsorption of Cd(II) and Zn(II) ions

3.2.1) Effect of pH

The pH value is one of the important factors in the adsorption process. It affects the degree of ionization of the metal ion species and the surface charge of adsorbent, all of that can lead to the different adsorption behavior and capacity. The effect of pH on the adsorption of Cd(II) and Zn(II) ions was determined to find the optimum pH for adsorption process. In aqueous solution, cadmium species can be presented as Cd^{2+}, $CdOH^{+}$, $Cd(OH)_2$ and $Cd(OH)_3^-$. The distribution of these cadmium species depends on the pH of solution. In the pH range studied (pH 2 − 6), cadmium was found as free ions (Cd^{2+}), no precipitation occurred [82-83]. Similarly to zinc, zinc species in aqueous solution mainly existed in the Zn^{2+} form (>99.8%) whereas the presence of hydrolyzed form was lower than 0.2% at the pH range studied [21]. Fig. 3.4 demonstrates the adsorption of Cd(II) and Zn(II) onto leonardite with the initial metal concentration of 30 mg/L at the pH range of 2 − 6. Adsorption of both metals was found to be strongly dependent on pH value. In strong acidic condition (pH 2 − 3), the adsorbed amounts of Cd(II) and Zn(II) were relatively low. Metal ions can be adsorbed around 6% for Cd(II) and 3% for Zn(II). This can be described by protonation of functional groups found in

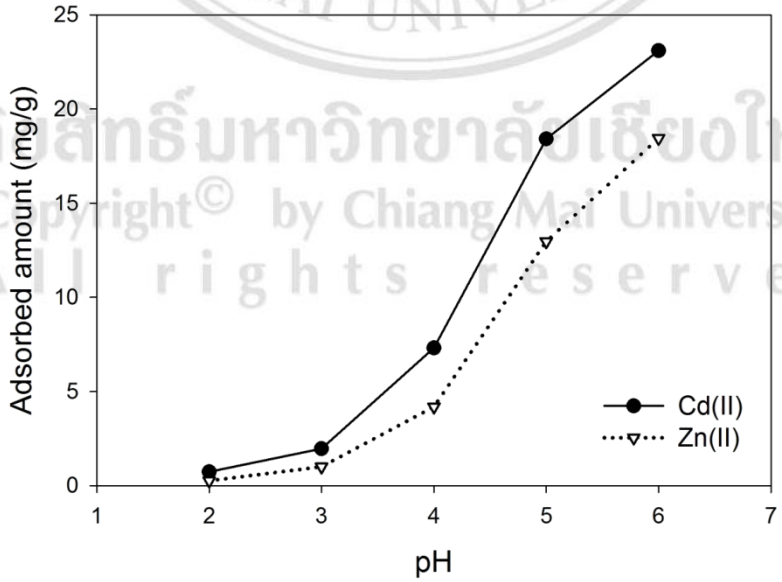

Fig. 3.4 Effect of pH on the individual adsorption of Cd(II) and Zn(II) on leonardite (initial metal concentration 30 mg/L, 30 °C, 5 h)

leonardite. According to FTIR result, various types of functional group were found in leonardite such as carboxyl, phenolic groups of humic substances and silanol group of inorganic matter. The dissociation of these functional groups can be controlled by solution pH. Carboxyl groups start to dissociate protons at slightly acidic up to neutral region [84]. Silanol groups dissociate at above pH 4 [85]. Thus, at low pH values, most of functional groups are protonated. Less active site is available for adsorption of metal ions leading to poor adsorption. Moreover, at low pH, the solution contains high concentration of hydrogen ions which can hinder the adsorption of metal ions. Phenolic groups are not expected to cooperate with metal ions in the pH range studied because the dissociation starts at pH 9 [86].

As the pH increases, more dissociation of functional groups takes place and the negatively charged sites of leonardite surface increase. The concentration of hydrogen ions in the solution also decreases. Therefore, metal ions can be more adsorbed. The deprotonation reactions of binding sites of leonardite are described by equation (3.1) and (3.2).

$$\text{R-COOH} \rightleftharpoons \text{R-COO}^- + \text{H}^+ \quad (3.1)$$

$$\equiv\text{SiOH} \rightleftharpoons \equiv\text{SiO}^- + \text{H}^+ \quad (3.2)$$

The metal uptake equations for deprotonated functional groups are described by equation (3.3) and (3.4).

$$\text{R-COOH} + \text{M}^{2+} \rightleftharpoons [\text{R-COOM}]^+ + \text{H}^+ \quad (3.3)$$

$$\equiv\text{SiOH} + \text{M}^{2+} \rightleftharpoons \equiv\text{SiOM}^+ + \text{H}^+ \quad (3.4)$$

Adsorbed amount of Cd(II) and Zn(II) increased with increasing pH. The significant change of the adsorbed amount was observed at pH > 3, which corresponded to the deprotonation of the functional groups. The maximum adsorbed amount of Cd(II) and Zn(II) were observed at pH 6. The adsorption capacity was 23.10 mg/g or 74.6% for Cd(II) and 18.44 mg/g or 61.5% for Zn(II). From the results, pH 6 was the suitable pH for adsorption of Cd(II) and Zn(II) on leonardite and was applied in further experiments.

3.2.2) Effect of contact time

In order to study the influence of time on the adsorption of Cd(II) and Zn(II) ions on leonardite, adsorption of the two metals at 10, 20, 30, 40, 50, 60, 90, 120, 180, 240, and 300 min was investigated. The adsorption was conducted at pH 6, the temperature of 30 °C, and the initial metal concentration of 30 mg/L. The relationship between contact time and metal ions uptake by leonardite is shown in Fig. 3.5. It was found that Cd(II) rapidly adsorbed on leonardite at the initial contact time. After 10 min, the adsorption process proceeded slowly. No significant change was observed after 60 min. In the case of Zn(II), it also quickly adsorbed within 10 min. After that, very small adsorbed amount increased with increasing contact time. Hence, the contact time of 60 min was considered as equilibrium time for adsorption of both Cd(II) and Zn(II) onto leonardite and was used in the further adsorption experiments.

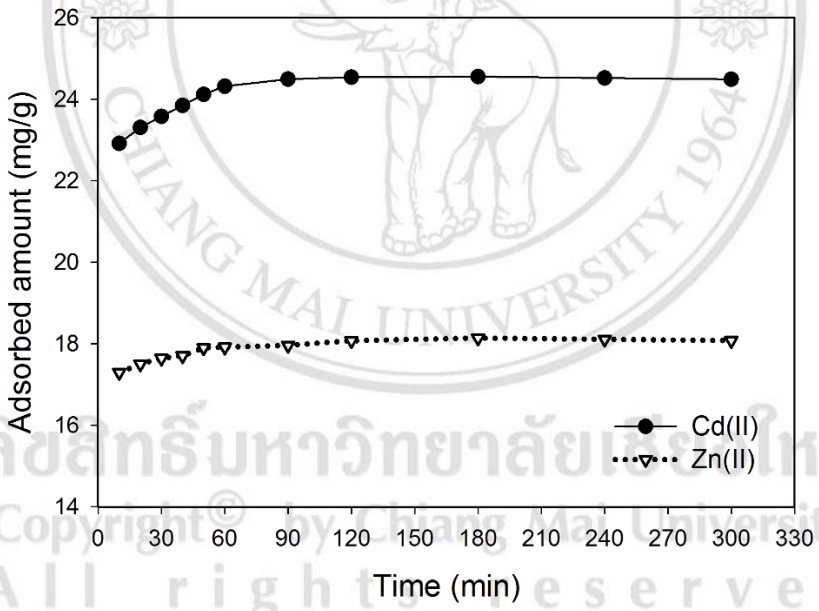

Fig. 3.5 Effect of contact time on the individual adsorption of Cd(II) and Zn(II) on leonardite (initial metal concentration 30 mg/L, 30 °C, pH 6)

3.2.3) Adsorption kinetics

In order to describe the kinetic of Cd(II) and Zn(II) adsorption process, the experimental data of Cd(II) and Zn(II) as the function of time were analyzed by 3 kinetic models: pseudo first order, pseudo second order, and intra-particle diffusion models.

3.2.3.1) Pseudo first order model

The pseudo first order equation is given by:

$$\frac{dq_t}{dt} = k_1(q_e - q_t) \tag{3.5}$$

Integration and rearranged in linear form:

$$\log(q_e - q_t) = \log q_e - \frac{k_1}{2.303}t \tag{3.6}$$

If the plot of $\log(q_e - q_t)$ versus t lies on the straight line, the adsorption system will follow the pseudo-first-order kinetic. The pseudo-first-order rate constant, k_1 (min^{-1}) and equilibrium adsorbed amount, q_e (mg/g) can be calculated from slope and intercept of the plot, respectively.

Fig. 3.6 shows the plot of pseudo first order kinetic for the adsorption of Cd(II) and Zn(II) on leonardite for the initial time of 60 min. It can be observed that the plots of Cd(II) and Zn(II) deviated from the straight line. The values of k_1, calculated q_e and the correlation coefficient (R^2) are presented in Table 3.4. The R^2 values of Cd(II) and Zn(II) were 0.9500 and 0.9191, respectively. These values were considerably high but the calculated q_e values for both metals were much lower than experimental q_e values. The calculated q_e values of Cd(II) and Zn(II) were 2.85 and 1.46 mg/g, respectively whereas the q_e values of Cd(II) and Zn(II) obtained from the experiments were 24.49 and 17.96 mg/g. This indicated that pseudo-first order model was not applicable for adsorption of Cd(II) and Zn(II) on leonardite.

3.2.3.2) Pseudo second order model

The pseudo second order equation can be represented in the following form:

$$\frac{dq_t}{dt} = k_2(q_e - q_t)^2 \tag{3.7}$$

Integration and rearranged the equation, it gives:

$$\frac{t}{q_t} = \frac{1}{k_2 q_e^{\,2}} + \frac{t}{q_e} \tag{3.8}$$

The pseudo second order rate constant, k_2 (g/mg/min) and equilibrium adsorbed amount, q_e can be determined from slope and intercept of plot of the t/q_t against t.

The pseudo second order kinetic plots for the adsorption of Cd(II) and Zn(II) by leonardite (Fig. 3.7) show a straight-line pattern results. Parameters and correlation coefficient of pseudo second order kinetic were listed in Table 3.4. The R^2 values for Cd(II) and Zn(II) were 0.9998 and 0.9999, respectively. The calculated q_e values were very close to the experimental q_e values. The high correlation coefficients and the good agreement between the calculated and the experimental q_e suggested that the adsorption of Cd(II) and Zn(II) on leonardite followed the pseudo-second order model. The rate constant, k_2, of Cd(II) and Zn(II) were 0.0377 and 0.0897 g/mg/min, respectively. The lower of k_2 value indicated that adsorption rate of Cd(II) was greater than that of Zn(II). The pseudo-second order model is based on the assumption that the adsorbate was adsorbed onto two surface sites [87].

3.2.3.3) Intra-particle diffusion model

Since the pseudo first order kinetic and the pseudo second order kinetic do not describe the adsorption mechanism. Thus, the intra-particle diffusion model was applied. The intra-particle diffusion model is expressed as:

$$q_t = k_{id} t^{0.5} + C \tag{3.9}$$

If the plot of q_t versus $t^{0.5}$ gives a straight line passing through the origin, then the adsorption process is controlled by intra-particle diffusion only. However, if the data

exhibit multi-linear plots, then two or more steps influence the adsorption process. The slope of the plot gives the value of the intra-particle diffusion rate constant, k_{id} (mg/g/min$^{0.5}$), and intercept gives the value of the constant related to the thickness of boundary layer, C (mg/g).

Fig. 3.8 presents the plots of Cd(II) and Zn(II) uptake against $t^{0.5}$. Plots of both Cd(II) and Zn(II) deviated from the origin and exhibited two types of linearity indicating two diffusion process. The first, sharper stage can be attributed to the diffusion of metal ions through the solution to the external surface of the leonardite or the boundary layer diffusion of the metal ions. The second stage can be attributed to the final equilibrium for which the intra-particle diffusion starts to slow down due to extremely low metal concentration left in solution. It can be suggested that the adsorption of Cd(II) and Zn(II) might be controlled by both film and intra-particle diffusions. The intra-particle diffusion parameters and R^2 values are shown in Table 3.4. The R^2 values of Cd(II) and Zn(II) were 0.6771 and 0.7516, respectively. These values were slightly low since the plots were separated into two straight lines.

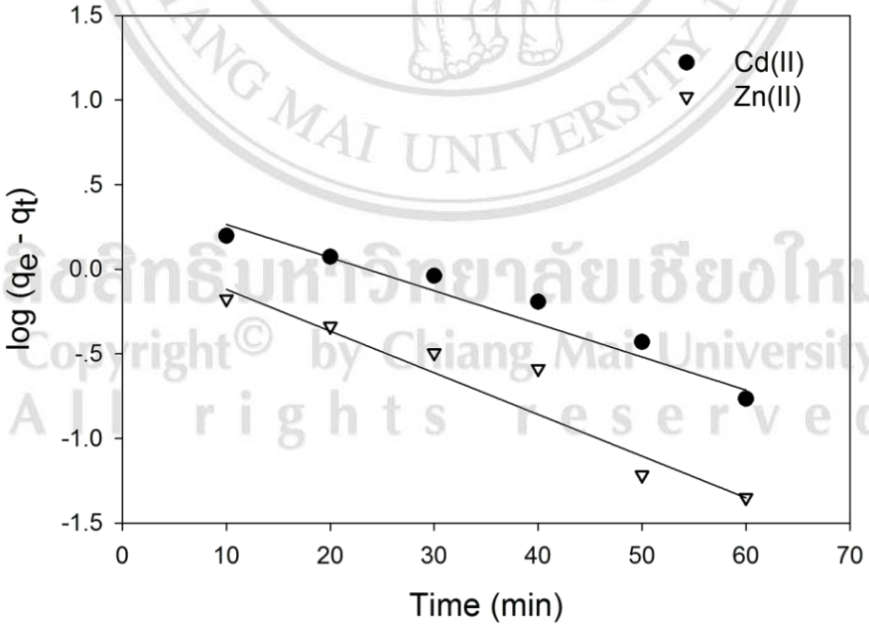

Fig. 3.6 Pseudo first order plot for the adsorption of Cd(II) and Zn(II) on leonardite

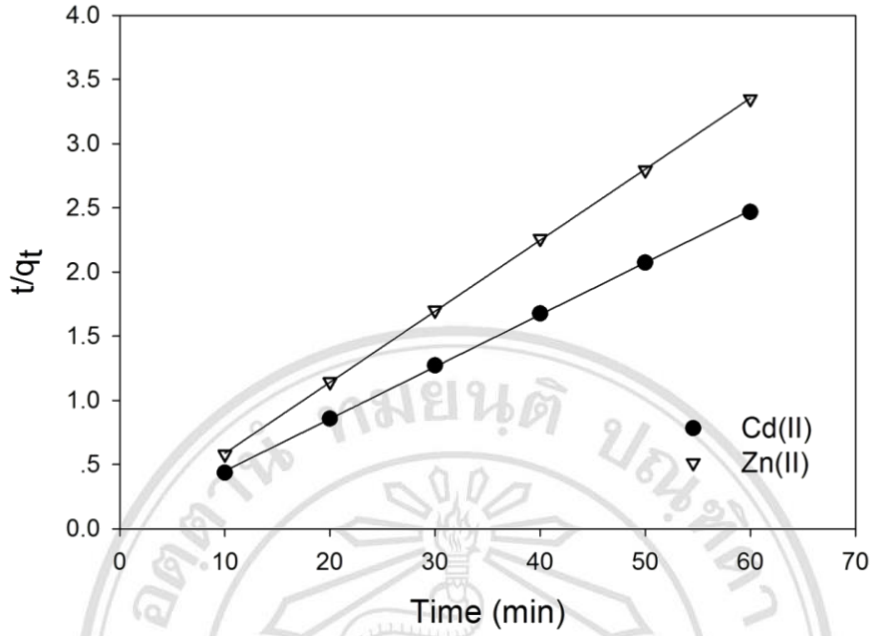

Fig. 3.7 Pseudo second order plot for the adsorption of Cd(II) and Zn(II) on leonardite

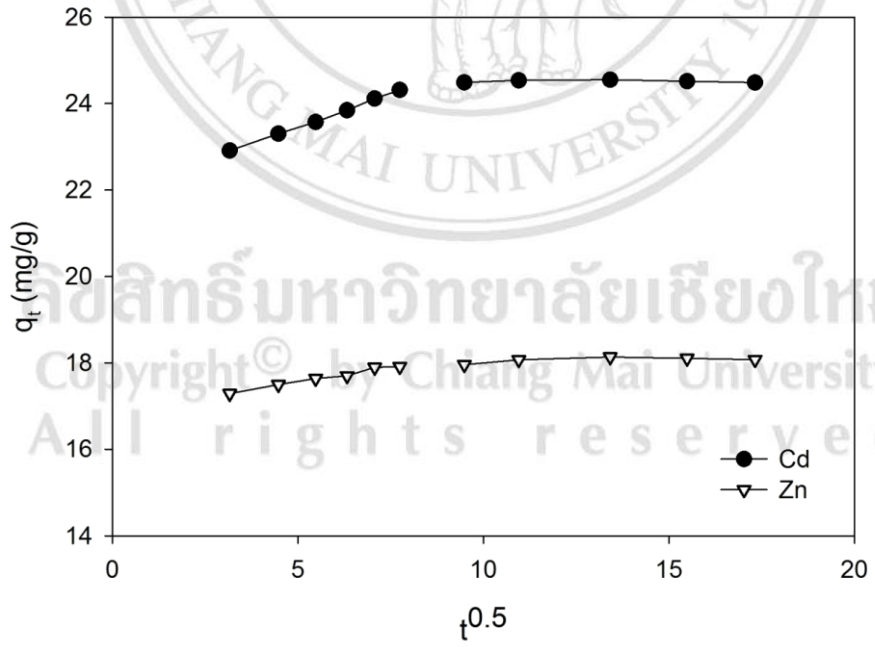

Fig. 3.8 Intra-particle diffusion plot for the adsorption of Cd(II) and Zn(II) on leonardite

Table 3.4 Kinetic parameters for Cd(II) and Zn(II) adsorption onto leonardite

Kinetic model	Cd(II)	Zn(II)
q_e, exp (mg/g)	24.49	17.96
Pseudo first order		
q_e, cal (mg/g)	2.85	1.46
k_1 (min^{-1})	0.0415	0.0553
R^2	0.9500	0.9191
Pseudo second order		
q_e, cal (mg/g)	24.63	18.08
k_2 (g/mg/min)	0.0377	0.0897
R^2	0.9998	0.9999
Intra-particle diffusion		
k_{id} ($mg/g/min^{0.5}$)	0.102	0.0519
C (mg/g)	23.12	17.37
R^2	0.6771	0.7516

3.2.4) Adsorption isotherm

Generally, adsorption isotherm is used to describe the relation between the amount of adsorbate adsorbed by adsorbent and amount of adsorbate remaining in the medium at equilibrium and constant temperature. The adsorption isotherms of Cd(II) and Zn(II) in the single component system were studied at pH 6, contact time of 60 min, temperature of 30 °C, and the initial metal concentration of 5 − 50 mg/L.

The adsorption isotherms for the individual adsorption of Cd(II) and Zn(II) on leonardite are shown in Fig. 3.9. The equilibrium adsorbed amount increased with the increasing metal concentration. It can be observed that the isotherm curves of Cd(II) and Zn(II) are quite different. The Cd(II) isotherm curve increased more rapidly with increasing metal concentration. As the metal concentration increased, the difference in the magnitude of adsorbed amount between Cd(II) and Zn(II) increased.

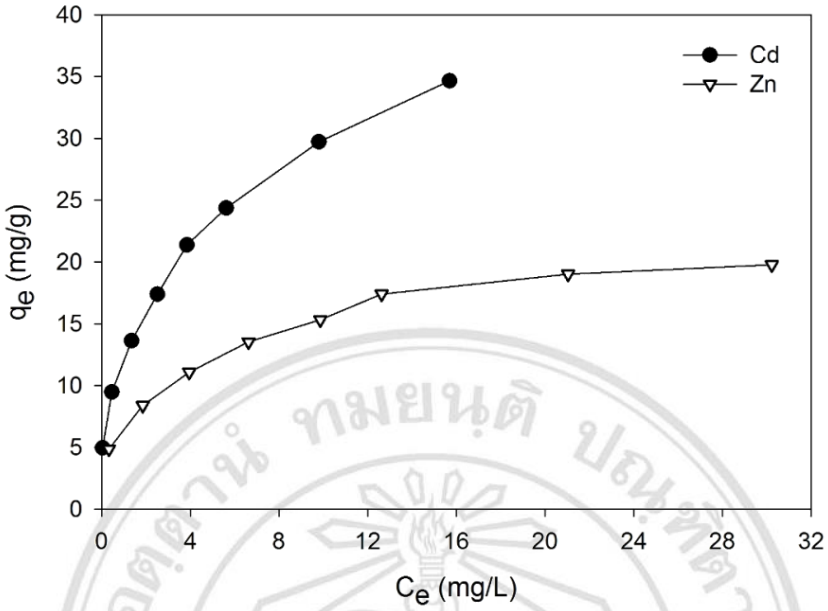

Fig. 3.9 Individual adsorption isotherm of Cd(II) and Zn(II)
(initial metal concentration 5 − 50 mg/L, pH 6, 60 min, 30 °C)

The equilibrium adsorption data were then studied using Langmuir isotherm and Freundlich isotherm.

(1) *Langmuir isotherm model*

The Langmuir isotherm equation is expressed by the following empirical equation:

$$q_e = \frac{q_m b C_e}{1 + b C_e} \tag{3.10}$$

where q_m (mg/g) is the maximum adsorption capacity of adsorbent and b (L/mg) is Langmuir constant related to adsorption intensity. This equation can be linearized as follows:

$$\frac{C_e}{q_e} = \frac{1}{q_m b} + \frac{C_e}{q_m} \tag{3.11}$$

The parameters q_m and b can be calculated from, respectively, the slope and the intercept of the plot of C_e against C_e/q_e. If the R^2 value of the plot is close to 1, it can be suggested that the adsorption data satisfy Langmuir isotherm.

(2) *Freundlich isotherm model*

The Freundlich isotherm equation is given:

$$q_e = K_F C_e^{1/n} \tag{3.12}$$

The linear form of Freundlich isotherm equation is:

$$\log q_e = \log K_F + \frac{1}{n} \log C_e \tag{3.13}$$

where K_F and *1/n* are the Freundlich constants related to adsorption capacity and heterogeneity, respectively. If the plotting of log q_e and log C_e yields a straight line, the adsorption data fit to the Freundlich isotherm. If the *1/n* value approaches 0, the heterogeneity of the adsorption site increases. On the other hand, if the *1/n* value approaches 1, the homogeneity of the adsorption site increases [88].

In this research, the analysis of adsorption isotherm was performed using linear regression and non-linear regression methods. In the linear regression method, the isotherm equation was arranged to linear form. Then, the adsorption data was plotted. The applicability of isotherm models can be evaluated by correlation coefficient (R^2). The isotherm parameters can be obtained from slope and intercept of the plot. In the non-linear regression method, the isotherm equation was used in the original form and the error function is required. The error function was used to measure the difference between experimental data and data predicting by isotherm model. The adsorption isotherm parameters were determined by minimizing the value of error function using Solver tool in Microsoft Excel. In this work, five error functions were applied including root mean square error (RMSE), the sum of the squares of the errors (ERRSQ), mean absolute percentage error (MAPE), Marquardt's percent standard deviation (MPSD) and chi-square analysis (χ^2). The fit of adsorption isotherm was evaluated from the isotherm model which provided the lowest error value.

3.2.4.1) Cd(II)

(1) *Linear regression method*

Linear plots of Langmuir isotherm and Freundlich isotherm of Cd(II) are demonstrated in Figs. 3.10 and 3.11, respectively. As seen, Langmuir plot showed the little deviation from the linearity whereas Freundlich plot showed the linearity of the plot. The isotherm parameters of Langmuir and Freundlich equations, together with the correlation coefficient (R^2), are given in Table 3.5. The R^2 values of Langmuir and Freundlich isotherm were 0.9684 and 0.9942, respectively. The Freundlich isotherm appeared to be the good model for adsorption of Cd(II) in term of the higher of R^2 value. The Freundlich isotherm parameter, K_F and $1/n$ were 13.14 and 0.344, respectively. $1/n$ value became closer to zero suggested the heterogeneity surface of leonardite. The Cd(II) adsorption capacity of leonardite obtained from Langmuir isotherm were 37.04 mg/g.

(2) *Non-linear regression method*

The isotherm parameters of Langmuir and Freundlich equations determined by the non-linear regression method using 5 error functions, together with the error values are given in Table 3.5. It was found that the Freundlich isotherm provided the lower error values than that of Langmuir isotherm for all error analysis. Thus, it can be suggested that the adsorption of Cd(II) fitted to Freundlich isotherm. Both linear and non-linear regression methods indicated the fit of Freundlich isotherm. These results confirmed the applicability of Freundlich isotherm for describing the Cd(II) adsorption data.

Each error function gave its own isotherm parameter set. The Freundlich isotherm parameter sets (K_F and $1/n$) obtained from non-linear regression were quite similar to those of linear regression method. Conversely, some Langmuir isotherm parameter sets (q_m and b) obtained from non-linear regression method were different from those of linear regression. Among the isotherm parameter sets determined by non-linear regression, it was observed that the isotherm parameter sets derived by RMSE and ERRSQ were similar.

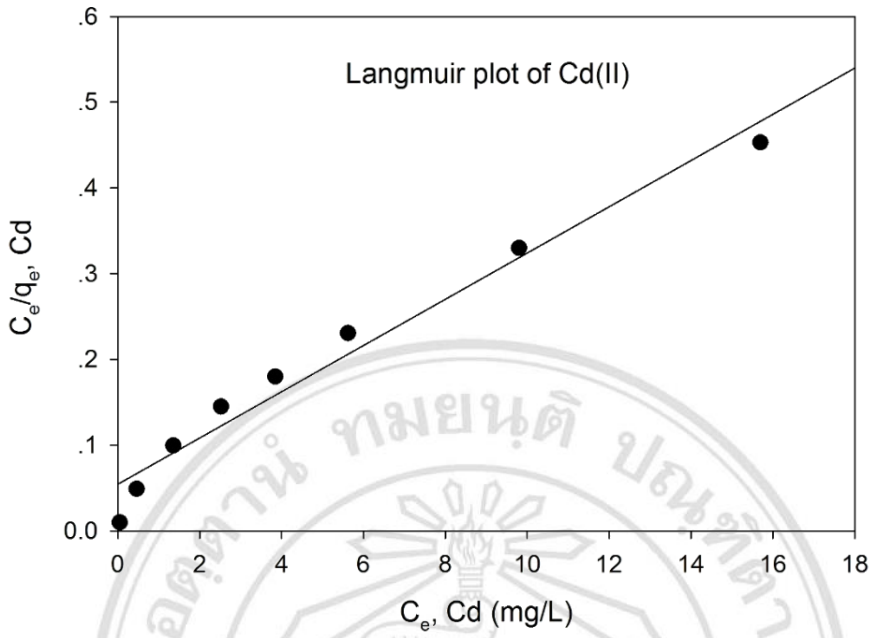

Fig. 3.10 Linear plot of Langmuir isotherm of Cd(II)

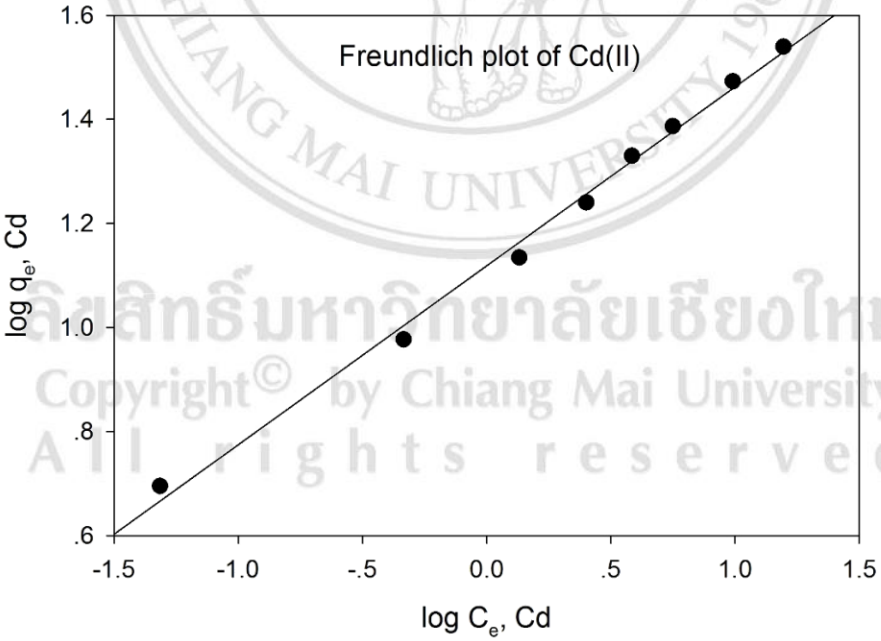

Fig. 3.11 Linear plot of Freundlich isotherm of Cd(II)

Table 3.5 Adsorption isotherm parameters for Cd(II) adsorption

Adsorption isotherm	Parameter	Linear regression	Non-linear regression				
			RMSE	ERRSQ	MAPE	MPSD	χ^2
Langmuir							
	q_m (mg/g)	37.04	38.26	38.26	32.50	34.03	27.76
	b (L/mg)	0.496	0.374	0.374	0.533	0.553	1.86
	R^2	**0.9684**					
	RMSE	2.655	**2.311**	2.311	2.865	2.572	4.610
	ERRSQ	56.41	42.72	**42.72**	65.66	52.93	170.03
	MAPE	21.42	19.72	19.72	**18.67**	19.87	27.33
	MPSD	96.96	96.96	96.96	96.97	**92.87**	128.02
	χ^2	21.56	29.91	29.91	23.78	20.73	**10.37**
	SNE	3.170	3.232	3.232	3.243	**3.015**	4.347
Freundlich							
	K_F	13.14	12.77	12.77	12.93	12.91	12.98
	1/n	0.344	0.366	0.366	0.358	0.359	0.356
	R^2	**0.9942**					
	RMSE	0.697	**0.472**	0.472	0.497	0.493	0.508
	ERRSQ	3.888	1.783	**1.783**	1.974	1.944	2.062
	MAPE	4.222	3.726	3.726	**3.715**	3.715	3.742
	MPSD	19.32	17.29	17.29	16.80	**16.79**	16.88
	χ^2	0.220	0.197	0.197	0.175	0.176	**0.174**
	SNE	5.000	3.809	3.809	3.767	**3.758**	3.812

In order to select the optimum isotherm parameter set, "sum of normalized errors, SNE" was considered. By this calculation method, each isotherm parameter set was tested to all error functions to yield the error values for each error function. The obtained error values were divided by the maximum errors for that error function, and the results for each error function were combined as SNE value. The isotherm parameter set that yielded the smallest SNE value was considered as the optimum isotherm parameter set. The SNE values are shown in Table 3.5.

In the case of Langmuir isotherm, the order of SNE value was MPSD < linear regression < RMSE ~ ERRSQ < MAPE < χ^2. The SNE value for each method was slightly difference except the SNE value of chi-square. Error function "chi-square" had the highest SNE value and the determined isotherm parameter set differed from other methods. It may be stated that chi-square method failed to analyzed the Cd(II) adsorption data for Langmuir isotherm. The parameter set obtained from MPSD yielded the smallest SNE value. The q_m and b obtained from MPSD were 34.03 mg/g and 0.553 L/mg, respectively, whereas the q_m and b obtained from linear regression method were 37.04 mg/g and 0.496 L/mg, respectively. The comparison of adsorption data obtained from experiment, Langmuir model (linear regression) and Langmuir model (non-linear regression, MPSD) is presented in Fig. 3.12. As seen, adsorption data predicting by Langmuir isotherm was not agree with the Cd(II) experimental data. The result obtained from linear regression differed from non-linear regression (MPSD) as the metal concentration increased.

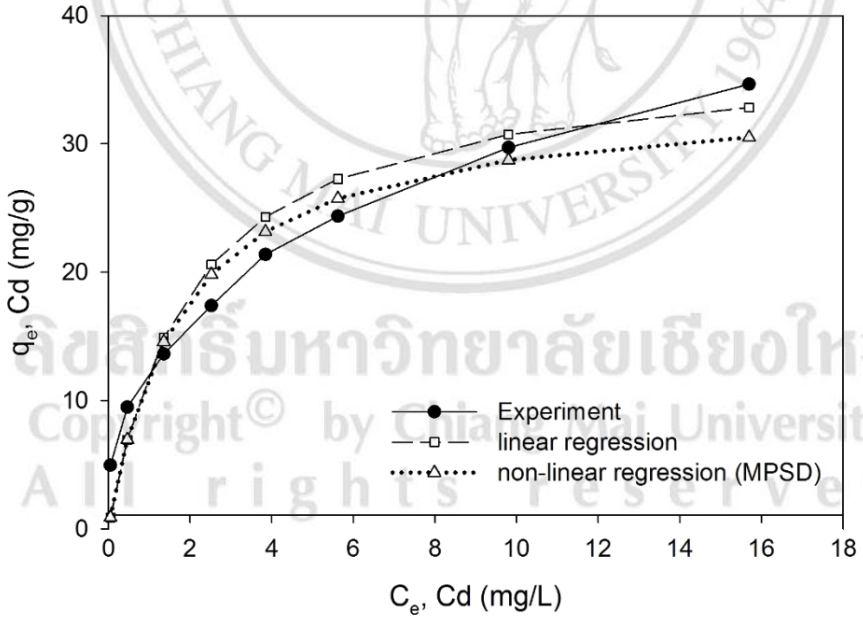

Fig. 3.12 The comparison of Cd(II) adsorption data obtained from experiment and Langmuir model (linear regression and non-linear regression, MPSD)

In the case of Freundlich isotherm, the order of SNE value was MPSD < MAPE < RMSE ~ ERRSQ < χ^2 < linear regression. The SNE value of each method was very close to each other, except the SNE value of the linear regression method. Although the linear regression method had the highest SNE value, the determined isotherm parameter set was similar to the other methods. Therefore, it may be assumed that all 6 methods provided the good results. The best parameter set was obtained using MPSD since it exhibited the lowest SNE value. It means that the Freundlich isotherm parameter set obtained from MPSD provided the fit closet to the experimental data. The K_F and $1/n$ obtained from MPSD were 12.91 and 0.359, respectively, whereas the K_F and $1/n$ obtained from linear regression method were 13.14 mg/g and 0.344, respectively. The comparison of adsorption data obtained from experiment, Freundlich model (linear regression) and Freundlich model (non-linear regression, MPSD) is presented in Fig. 3.13. The results of both linear regression and non-linear regression (MPSD) agreed well with the Cd(II) experimental data. It was observed that the calculating adsorption data using parameter set from MPSD was more close to the experimental data.

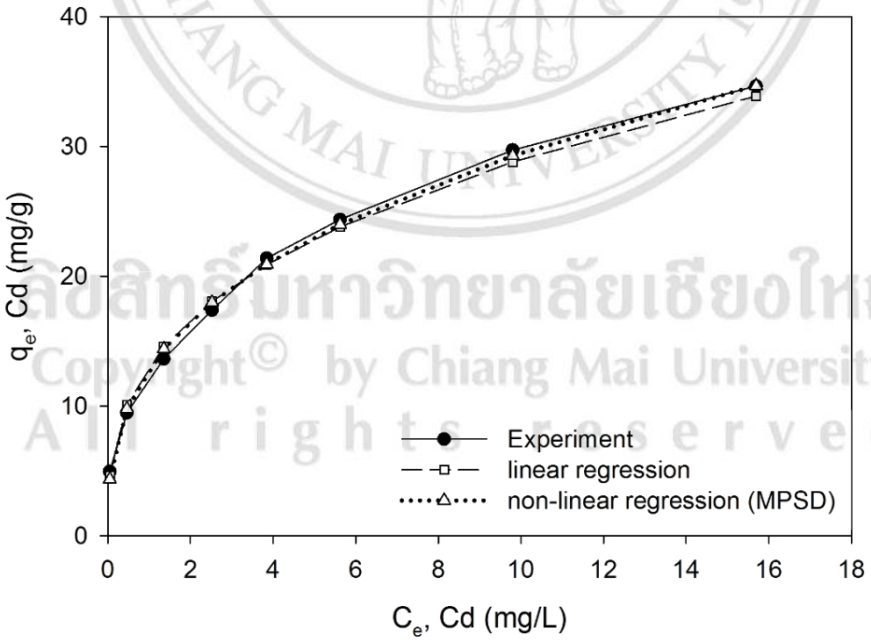

Fig. 3.13 The comparison of Cd(II) adsorption data obtained from experiment and Freundlich model (linear regression and non-linear regression, MPSD)

3.2.4.2) Zn(II)

(1) *Linear regression method*

Linear plots of Langmuir isotherm and Freundlich isotherm of Zn(II) are shown in Figs. 3.14 and 3.15, respectively. Both Langmuir and Freundlich plots slightly deviated from the linearity. The Zn(II) isotherm parameters of Langmuir and Freundlich equations, together with the R^2 values are given in Table 3.6. Both Langmuir and Freundlich isotherms showed a good fit to the Zn(II) experimental data with the R^2 of 0.9921 for Langmuir isotherm, and R^2 of 0.9905 for Freundlich isotherm. Langmuir isotherm had a little more R^2 value than Freundlich isotherm. The q_m and b of Zn(II) adsorption were 21.46 mg/g and 0.337 L/mg, respectively. The K_F and $1/n$ were 7.07 and 0.326, respectively.

(2) *Non-linear regression method*

The Zn(II) isotherm parameters of Langmuir and Freundlich equations determined by the non-linear regression method using 5 error functions, together with the error values, and the SNE values are given in Table 3.6. The results obtained from the non-linear regression method opposed to those of the linear regression method. All error functions indicated that Freundlich isotherm was more fitted to the adsorption data with the lower error values.

The Langmuir isotherm parameter sets obtained from the non-linear regression method were quite similar to those obtained from the linear regression method except for the MPSD and chi-square, which gave the different values. The Freundlich isotherm parameter sets determined from non-linear regression method were quite similar to those of linear regression method. Among the isotherm parameter sets determined by non-linear regression, the isotherm parameter sets derived by RMSE and ERRSQ were similar.

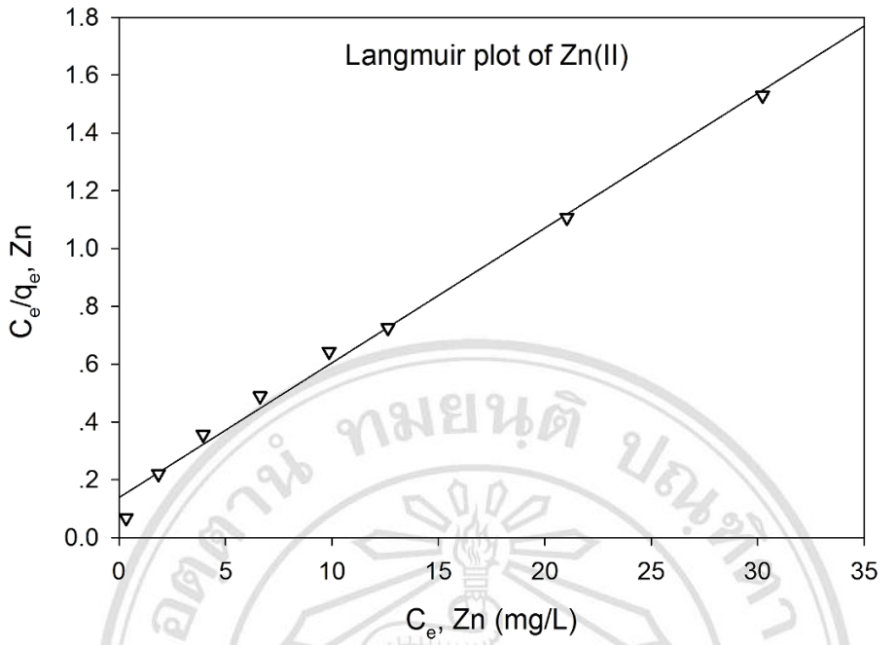

Fig. 3.14 Linear plot of Langmuir isotherm of Zn(II)

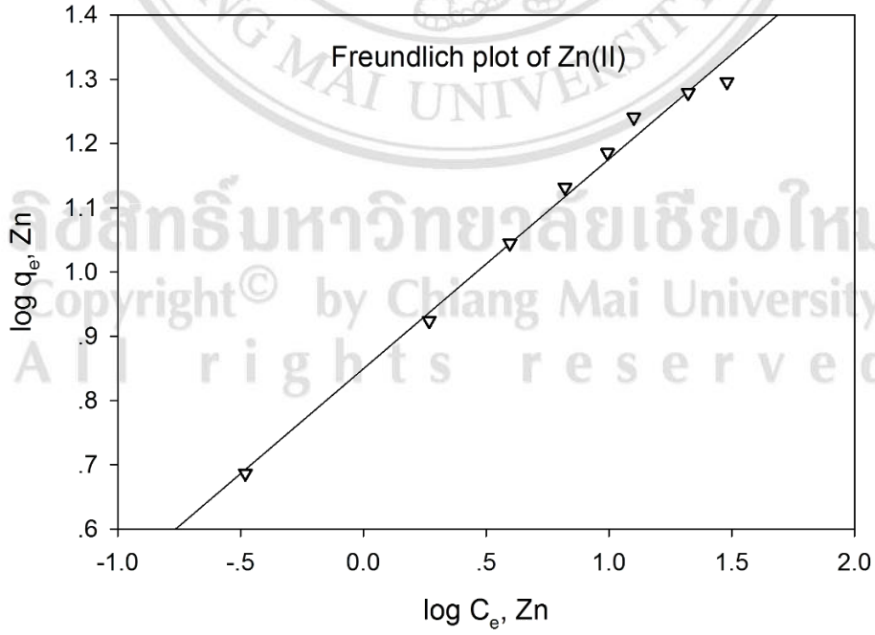

Fig. 3.15 Linear plot of Freundlich isotherm of Zn(II)

Table 3.6 Adsorption isotherm parameters for Zn(II) adsorption

Adsorption isotherm	Parameter	Linear regression	Non-linear regression				
			RMSE	ERRSQ	MAPE	MPSD	χ^2
Langmuir							
	q_m (mg/g)	21.46	21.31	21.31	21.34	19.78	18.65
	b (L/mg)	0.337	0.315	0.315	0.350	0.438	0.666
	R^2	**0.9921**					
	RMSE	1.216	**1.170**	1.170	1.235	1.298	1.674
	ERRSQ	11.84	10.96	**10.96**	12.19	13.48	22.41
	MAPE	10.94	11.30	11.30	**10.85**	12.19	14.51
	MPSD	55.56	56.02	56.02	55.33	**53.06**	58.43
	χ^2	3.727	4.238	4.238	3.524	2.743	**2.087**
	SNE	3.840	3.926	3.926	3.808	**3.773**	4.492
Freundlich							
	K_F	7.07	7.47	7.47	7.02	7.21	7.22
	1/n	0.326	0.302	0.302	0.332	0.312	0.317
	R^2	**0.9905**					
	RMSE	0.788	**0.715**	0.715	0.842	0.738	0.743
	ERRSQ	4.965	4.089	**4.089**	5.667	4.362	4.420
	MAPE	3.330	4.885	4.885	**3.200**	3.871	3.815
	MPSD	21.34	21.92	21.92	22.49	**20.70**	20.76
	χ^2	0.268	0.285	0.285	0.289	0.258	**0.257**
	SNE	4.369	4.532	4.532	4.655	**4.253**	4.256

In the case of Langmuir isotherm, the order of SNE values was MPSD < MAPE < linear regression < RMSE ~ ERRSQ < χ^2. SNE value of each method was close to each other, except the SNE value of χ^2. Error function "chi-square" had the highest SNE value and the determined isotherm parameter set differed from other methods. It may be stated that chi-square method failed to analyzed the Zn(II) adsorption data for Langmuir isotherm. The parameter set obtained from MPSD yielded the smallest SNE value. The q_m and b obtained from MPSD were 19.78 mg/g and 0.438 L/mg, respectively, whereas the q_m and b obtained from linear regression method were 21.46 mg/g and 0.337 L/mg, respectively. The comparison of adsorption data obtained from experiment, Langmuir model (linear regression), and Langmuir model (non-linear regression, MPSD) is presented in Fig. 3.16. As seen, some plots of the calculated data (both linear regression and non-linear regression) deviated from experimental data. Thus, it can be conclude that Langmuir isotherm moderately predicted the adsorption data of Zn(II). The result obtained from linear regression differed from non-linear regression (MPSD) as the metal concentration increased.

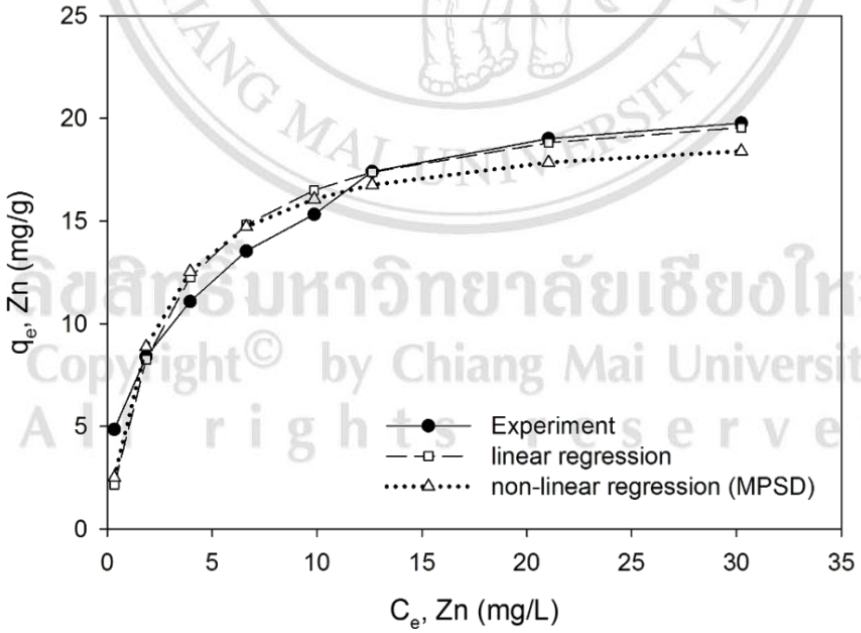

Fig. 3.16 The comparison of Zn(II) adsorption data obtained from experiment and Langmuir model (linear regression and non-linear regression, MPSD)

In the case of Freundlich isotherm, the order of SNE values was MPSD < χ^2 < linear regression < RMSE ~ ERRSQ < MAPE. SNE value of each method was slightly different. The MAPE had the highest SNE value but the determined isotherm parameter set was similar to the other methods. Therefore, it may be assumed that all 6 methods provided the good results. The best parameter set was obtained using MPSD. From MPSD, K_F and 1/n were 7.21 and 0.312, respectively, whereas the linear regression method gave the value of K_F and 1/n as 7.07 and 0.326, respectively. The comparison of adsorption data obtained from experiment, Freundlich model (linear regression), and Freundlich model (non-linear regression, MPSD) is presented in Fig. 3.17. The results of both linear regression and non-linear regression (MPSD) agreed quite well with the Zn(II) experimental data. Only two plots of calculated data deviated from the experimental data. The calculating adsorption data using parameter set from MPSD was close to the calculating adsorption data using parameter set from the linear regression method.

From all results, it can be said that adsorption of Zn(II) on leonardite fitted to both Langmuir isotherm and Freundlich isotherm but Freundlich isotherm is more favored.

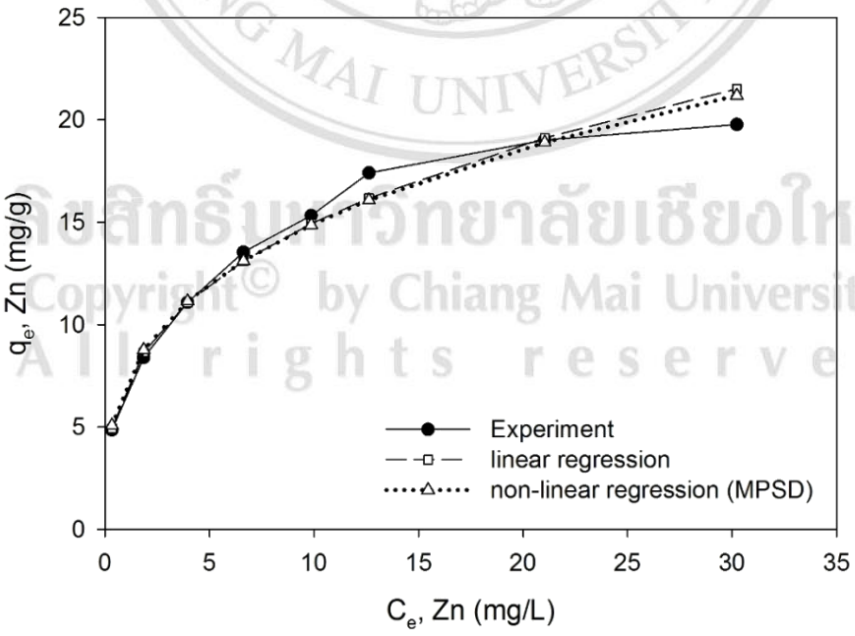

Fig. 3.17 The comparison of Zn(II) adsorption data obtained from experiment and Freundlich model (linear regression and non-linear regression, MPSD)

The adsorption of Cd(II) and Zn(II) on leonardite in the single component system are more favored to Freundlich isotherm. The Freundlich isotherm explains the adsorption on the heterogeneous surfaces. This corresponded to the surface property of leonardite. Leonardite composed of minerals and organic matters which bear the variety of functional groups. The surface of leonardite is expected to be the heterogeneous surface. Moreover, the isotherm curves of Cd(II) and Zn(II) were of Freundlich type since the adsorbed amount increased as long as there was the increase of the equilibrium metal concentration in the solution.

The comparison of adsorption capacity between leonardite and the other adsorbents for Cd(II) and Zn(II) is demonstrated in Table 3.7. It revealed that leonardite has a great capability for adsorption of Cd(II) and Zn(II).

Table 3.7 Comparison of adsorption capacity of adsorbents for Cd(II) and Zn(II)

Metal ion	Adsorbent	q_m (mg/g)	References
Cd(II)	Leonardite	34.03	This work
	Bottom ash	13.70	Sukpreabprom *et al.* [89]
	Activated carbon	46.88	Abdullah *et al.* [90]
	Moss	28.00	Martins *et al.* [91]
	Zeolite 4A	30.27	Purna Chandra Rao *et al.* [92]
	Ball clay	27.27	Rao and Kashifuddin [93]
	Green alga	46.09	Areco *et al.* [94]
	Calcite	18.52	Yavuz *et al.* [95]
Zn(II)	Leonardite	19.78	This work
	Bottom ash	14.50	Sukpreabprom *et al.* [89]
	Activated carbon	45.41	Abdullah *et al.* [90]
	Zeolite 4A	42.82	Rao *et al.* [92]
	Green alga	22.89	Areco *et al.* [94]
	Bone charcoal	24.50	Wilson *et al.* [96]
	Sugar beet pulp	17.78	Reddad *et al.* [97]
	Banana peel	5.80	Annadurai *et al.* [98]

Compared to Zn(II), adsorption of Cd(II) was more favorable with the Cd(II) and Zn(II) monolayer adsorbed amount, q_m, of 34.03 and 19.78 mg/g, respectively. The same trend was observed from Freundlich isotherm with the greater K_F value of Cd(II). Commonly, the affinity of metal ions to adsorbent depends on several factors such as adsorbent characteristics, ionic properties, adsorption conditions and adsorption mechanism. The ionic properties of Cd(II) and Zn(II) are shown in Table 3.8.

Many studies [22, 99-101] described that the affinity of metal ions to adsorbents may be due to the hydrated ion radius and hydration enthalpy. In aqueous solution, metal ions will bind with water molecules. The hydrated ion radius of Cd(II) was smaller than Zn(II) which lead to the greater adsorption of Cd(II) as compared to Zn(II). The hydration enthalpy can be also described the adsorption of metal ions. The hydration enthalpy is the amount of energy released when ion dissolves in water forming an infinitely dilute solution. It indicates the stability of hydrated ions and reflects the ease of metal ions interacts with the adsorbent surface. The stronger hydration enthalpy, the more metal ions are hydrated and the less they can interact with the surface. The hydrated Zn(II) is assumed to be stable than the hydrated Cd(II) since the hydration enthalpy of Zn(II) was more than that of Cd(II). For this reason, Zn(II) will have lesser accessibility to the surface of leonardite. Therefore, Cd(II) was expected to be more adsorbed than Zn(II).

The other factors for describing the higher affinity of Cd(II) to leonardite were the electronegativity and index covalent. The electronegativity is 1.69 for Cd(II) and 1.65 for Zn(II). The more electronegative metal ions, the more strongly attracted to the surface [102]. The same trend was obtained by Brady and Tobin [103]. They stated that

Table 3.8 Properties of metal ion

Properties	Metal ion	
	Cd(II)	*Zn(II)*
Ionic radius	0.95 Å	0.74 Å
Hydrated ion radius	4.26 Å	4.30 Å
Hydration energy	-1807 kJ/mol	-2046 kJ/mol
Electronegativity	1.69	1.65
Covalent index	2.71	2.13

the metal uptake values were correlated with the covalent index of metal ions. The covalent index was developed for relating the metal-complex stability constants to the properties of ions. It was computed using the expression Xm^2r, where Xm is the electronegativity, and r is the ionic radius. The greater the covalent index value, the greater of the potential to form the covalent bond with biological ligands. Since leonardite is composed of humic substances, this hypothesis is reasonable for this study. Pandey *et al.* [104] determined the stability constants of complexes formed between the humic acid (isolated from the soil) and metal ions. The stability constant (log K) of Cd-humic acid complexes is greater than that of Zn-humic acid complexes (2.78 for Cd(II) and 2.74 for Zn(II)). The higher of log K values confirm the more stable character of binding between Cd(II) ions and humic acid. The molar HA/metal ratio was found to be 0.53 for Cd(II) and 0.50 for Zn(II). Furthermore, several publishes about adsorption of Cd(II) and Zn on humic acid have confirmed the greater affinity of Cd(II) [105-107]. Due to the reasons described above, it may be said that the greater affinity of Cd(II) towards leonardite was due to its smaller hydrated ion radius, lower hydration energy, and higher electronegativity, index covalent, and stability constant. As the smaller hydrated ion, Cd(II) can be more accessible to the surface of leonardite. The higher hydration energy of Zn(II) as compared to Cd(II) resulted in the more hydration and stability of Zn(II) hydrated ion which made it less accessible to the surface. Since the Cd(II) has higher electronegativity, index covalent, and stability constant, Cd(II) will be more attracted to the surface of leonardite and the stability of Cd(II)-humic acid complexes is greater than that of Zn(II).

3.2.5) Adsorption mechanism

The FTIR spectra of leonardite, leonardite-Cd, and leonardite-Zn gave additional information about the change in the functional groups of leonardite in effect of the interactions with metal ions. The FTIR spectra of leonardite before and after the adsorption of Cd(II) and Zn(II) are presented in Fig. 3.18. The significant changes under metal ions influence are observed for the OH band around 3400 cm^{-1}. Intensity of this band of leonardite-Cd and leonardite-Zn decreased as compared to that of leonardite. This band is at 3406 cm^{-1} for leonardite. After the adsorption, it shifted to 3385 cm^{-1} for Cd(II), and 3417 cm^{-1} for Zn(II). The decrease and shift of the band can result from the binding of the metal ions by OH groups. The shift of band towards the higher frequency indicated the change in the coordination sphere of the complex. The shift of band towards the lower frequency provides evidence of a rearrangement of the molecules to another type of coordination [108]. The binding by OH groups and Cd(II) has been also confirmed by the drop of the bands attributed to different kinds of OH groups localized within area of 1033

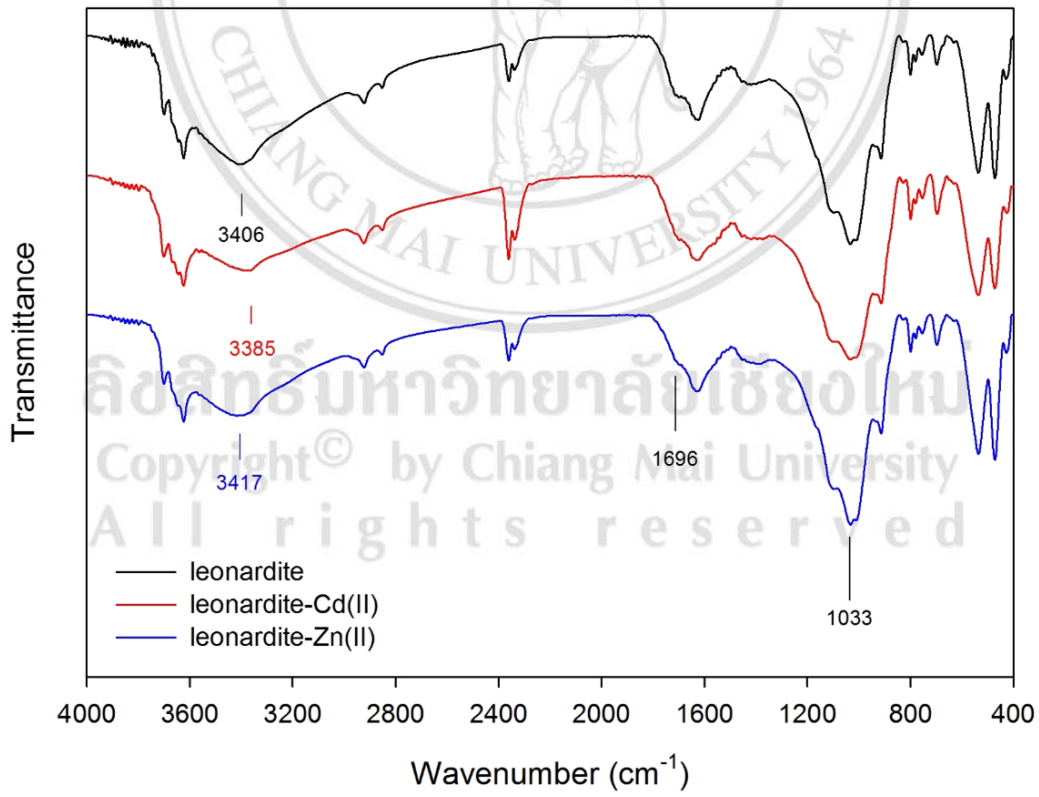

Fig. 3.18 The comparison of the FTIR spectra of leonardite, leonardite-Cd, and leonardite-Zn

– 1010 cm^{-1}. The adsorption of Cd(II) and Zn(II) are also formed with COOH contribution, visible as the decrease in the shoulder at ~1696 cm^{-1} (asymmetric stretching vibrations of C=O in COOH). The decrease of this band suggests that the COOH groups were converted to the COO- form [109].

The adsorption capability of leonardite is attributed to the clay minerals and organic matter in leonardite. The clay minerals are hydrous aluminium, magnesium or iron silicates. There are at least two majors possibilities as how to the surface negative charges of minerals are formed; (i) the hydroxyl groups including silanol (≡SiOH) and aluminol (≡AlOH) groups, which exist on the edge and on the outer layers of minerals can dispose of hydrogen which is the pH dependent process; (ii) the isomorphous ion replacement in the minerals, for example, Si^{4+} is substituted by Al^{3+} in the tetrahedral layer, Al^{3+} is substituted by Fe^{2+} or Mg^{2+} in the octahedral layer. The substituting ion has lesser charge than the true charge-neutralizing ion, thus there is charge imbalance. The negative charges, which appear as the result of isomorphous ion replacement, are pH independent and thus quite persistent [110]. Lackovic *et al.* [111] studied the adsorption of Cd(II) on illite. They reported that the reactions (3.14) – (3.16) best described the adsorption of Cd(II) on illite.

$$Cd^{2+} + SOH \rightleftharpoons SOCd^{+} + H^{+} \quad (3.14)$$

$$SOH + Cd^{2+} \rightleftharpoons SOH\cdots Cd^{2+} \quad (3.15)$$

$$Cd^{2+} + 2X^{-} \rightleftharpoons (X_2)^{2-}\cdots Cd^{2+} \quad (3.16)$$

where SOH represents the surface hydroxyl group, X^{-} represents the permanent negatively charged site resulting from isomorphous substitution. At low pH, adsorption involves a bidentate outer-sphere complex $(X_2)^{2-}\cdots Cd^{2+}$. Above pH 6, second outersphere complex involving SOH sites, $SOH\cdots Cd^{2+}$, plays significant role in adsorption, while at higher pH values (> 7.5), unidentate inner-sphere complex, $SOCd^{+}$, has increasing concentration, dominating adsorption at higher pH values. Gu and Evans [112] investigated the adsorption of Zn(II) on illite. They stated that two distinct adsorption mechanisms dominate the sorption of metals onto illite at different pH ranges: nonspecific ion-exchange reactions occurring in the lower pH range and specific inner-sphere surface complexation at the higher pH range.

For the part of organic matter, humic substances play the important role for the adsorption of Cd(II) and Zn(II) on leonardite. Xia *et al.* [113] studied the nature of binding sites of Zn(II) bound to soil humic substances. The best fit model for adsorption of Zn(II) on soil humic substances was obtained by using four O atoms and two S atoms in the first coordination shell. Two C atoms appeared in the second shell of Zn in soil humic substances. The appearance of C in the second shell confirmed that Zn formed inner-sphere complexes with humic substances. The distances of two S bond with Zn was 2.33 Å, and four O bond with Zn is 2.13 Å. The average distances of Zn···C was 3.29 Å for Chelex-extracted soil humic substances. Liu *et al.* [114] investigated the mechanism of the adsorption of Cd(II) on humic acid. It was found that Cd(II) enhanced aggregation of humic acid and finally raveled the spheroidal humic acid particles into the bean-like structure by coordinating to six O atoms of the functional groups of humic acid, with a Cd-O distance of 2.297 Å. Pandey *et al.* [104] reported that during metal-humic acid complex formation, 1 mol of humic acid complexed 2 mol of Cd(II) and Zn(II).

3.2.6) Effect of temperature

In order to study the effect of temperature on the equilibrium adsorption of Cd(II) and Zn(II) onto leonardite, the adsorption was investigated at the temperature of 10, 20, 30, and 40 °C. The experimental were performed at optimum conditions discussed in the previous sections. The adsorption isotherms of Cd(II) and Zn(II) at 10, 20, 30, and 40 °C are shown in Figs. 3.19 and 3.20, respectively. It can be observed that the adsorbed amount of both metals increased with the increase of temperature. It was suggested that the adsorption sites may increase due to the breaking of some external bonds near the edge of the particles as the temperature increase [115]. The adsorption data were then analyzed using Langmuir isotherm and Freundlich isotherm. Linear plots of Langmuir isotherm and Freundlich isotherm at 10, 20, 30, and 40 °C for Cd(II) are demonstrated in Figs. 3.21 and 3.22, respectively. From the results, Langmuir plots showed the deviation of adsorption data from linearity whereas Freundlich plots showed the good linearity of the plots for all temperature used. In the case of Zn(II), both Langmuir plots (Fig. 3.23) and Freundlich plots (Fig. 3.24) exhibited the linearity of the plots but there were the deviation of plots at low concentration for Langmuir plots, and at high concentration for Freundlich plots. The isotherm parameters, calculated using linear

regression and non-linear regression (MPSD), together with R^2 and error values are listed in Table 3.9.

For Cd(II), both R^2 and MPSD error values indicated that the adsorption data fitted to Freundlich isotherm for all the temperature. The K_F values increased from 11.44 to 13.87 (linear regression) as the temperature increased from 10 °C to 40 °C. The values of isotherm parameters obtained from linear regression and non-linear regression were not much different. The q_m values of Cd(II) slightly increased from 36.36 mg/g to 37.18 mg/g (linear regression) as the temperature increased. The magnitude of the increasing adsorbed amount was very small. Thus, it can be suggested that the temperature had low effect on the adsorption of Cd(II) on leonardite. For Zn(II), the R^2 values suggested that the adsorption data fitted well to Langmuir isotherm while the MPSD error values suggested the suitability of Freundlich isotherm. The increase in the temperature resulted in the increase of q_m values, as well the K_F values. Similar to Cd(II), the magnitude of the increasing adsorbed amount was very small. Therefore, it can be suggested that the temperature had low effect on the adsorption of Zn(II) on leonardite.

The adsorption of both Cd(II) and Zn(II) on leonardite were less affected by temperature. This is the good point for the application of this process for the wastewater treatment in Thailand. Generally, the water temperature is in the range of 10 – 40 °C in Thailand. From the point of view of process controls, there is no need to control the temperature of adsorption process in the real work environment in Thailand since this adsorption process can be performed in the temperature range of 10 – 40 °C with no significant change of adsorbed amount.

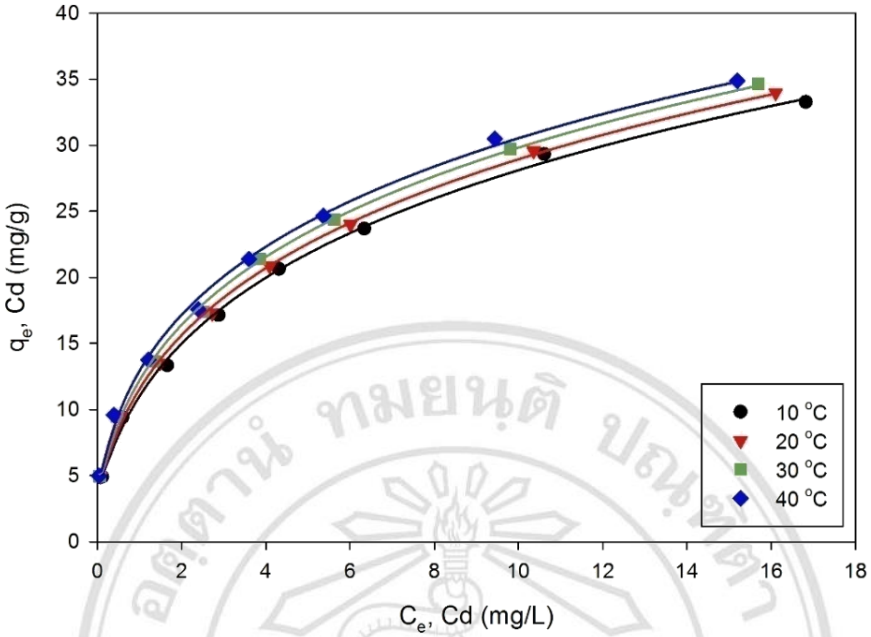

Fig. 3.19 Adsorption isotherms of Cd(II) on leonardite at 10, 20, 30, and 40 °C

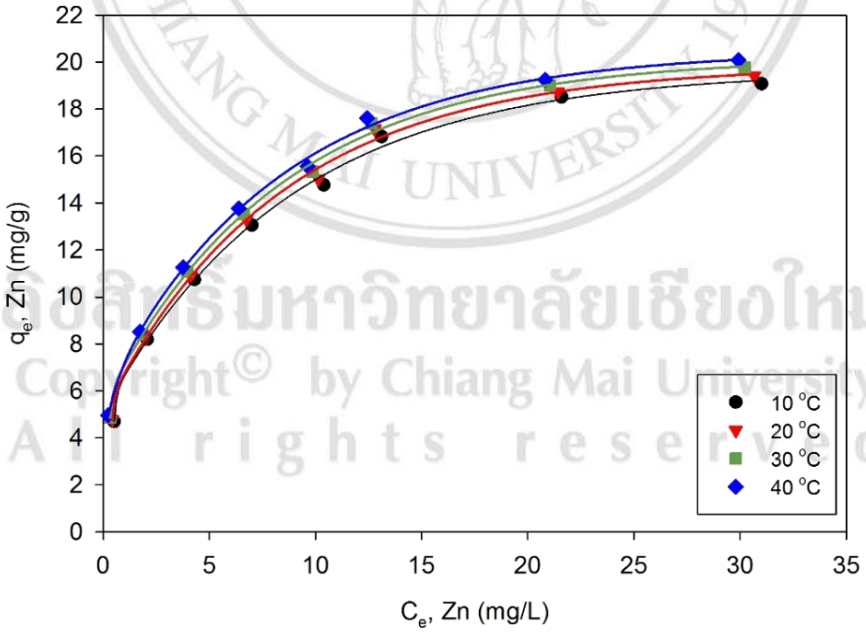

Fig. 3.20 Adsorption isotherms of Zn(II) on leonardite at 10, 20, 30, and 40 °C

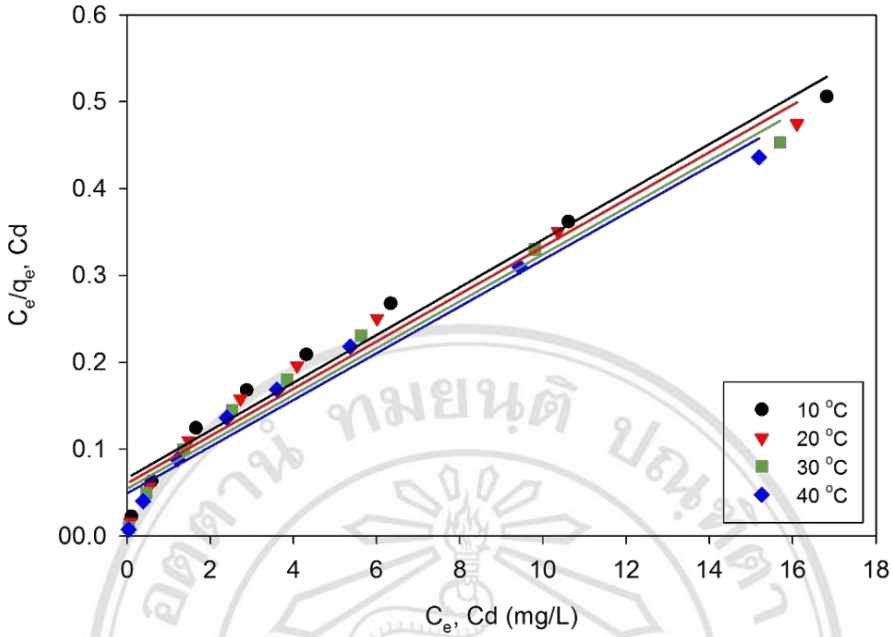

Fig. 3.21 Langmuir plots of Cd(II) at 10, 20, 30, and 40 °C

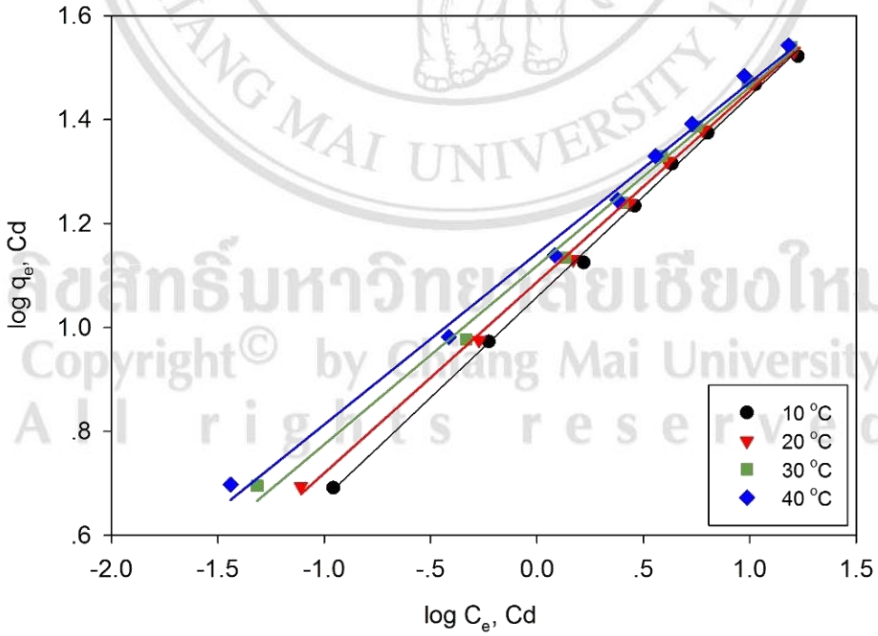

Fig. 3.22 Freundlich plots of Cd(II) at 10, 20, 30, and 40 °C

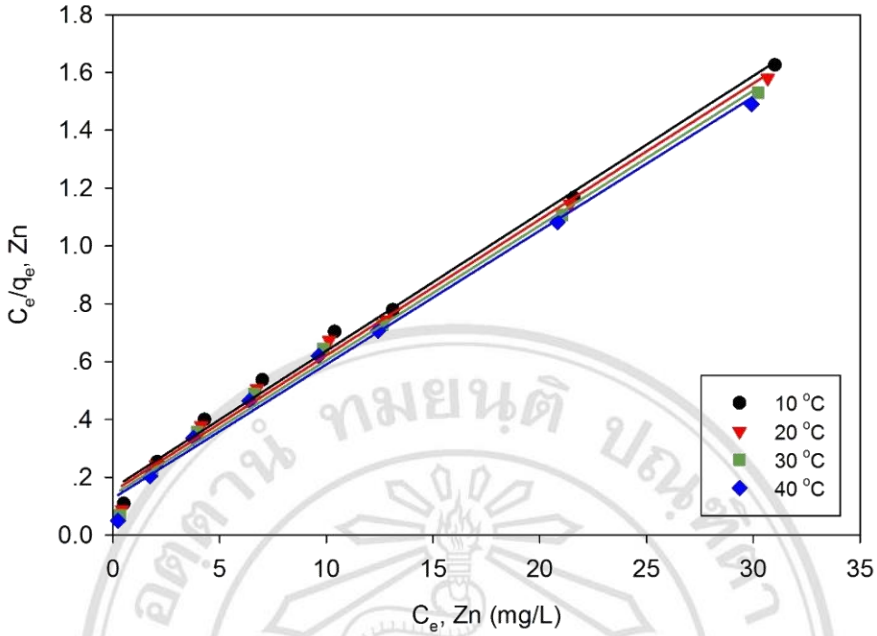

Fig. 3.23 Langmuir plots of Zn(II) at 10, 20, 30, and 40 °C

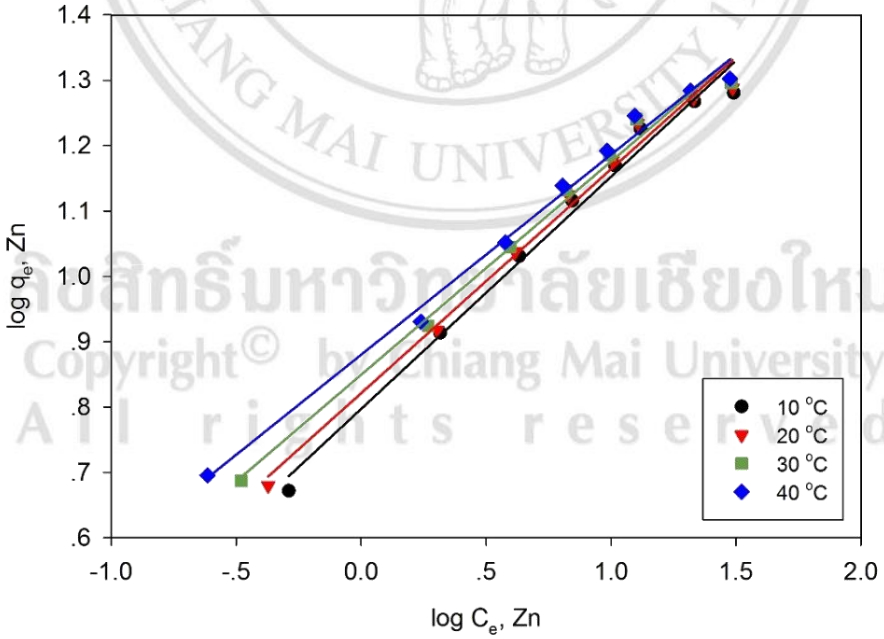

Fig. 3.24 Freundlich plots of Zn(II) at 10, 20, 30, and 40 °C

Table 3.9 Adsorption isotherm parameters for Cd(II) and Zn(II) adsorption at 10, 20, 30, and 40 °C

Adsorption isotherm	Metal ion	Temperature	Parameters					
			Linear regression			Non-linear regression		
Langmuir			q_m (mg/g)	b (L/mg)	R^2	q_m (mg/g)	b (L/mg)	MPSD
	Cd(II)	10 °C	36.36	0.414	0.9716	33.29	0.479	78.55
		20 °C	36.77	0.450	0.9691	33.48	0.522	85.45
		30 °C	37.04	0.496	0.9684	34.03	0.553	92.87
		40 °C	37.18	0.550	0.9693	33.75	0.633	99.09
	Zn(II)	10 °C	21.05	0.293	0.9933	19.66	0.363	40.03
		20 °C	21.23	0.313	0.9929	19.81	0.390	45.96
		30 °C	21.46	0.337	0.9921	19.78	0.438	53.06
		40 °C	21.60	0.364	0.9914	19.84	0.480	61.58
Freundlich			K_F	$1/n$	R^2	K_F	$1/n$	MPSD
	Cd(II)	10 °C	11.44	0.387	0.9986	11.44	0.387	11.85
		20 °C	12.22	0.368	0.9981	12.12	0.374	10.54
		30 °C	13.14	0.344	0.9942	12.91	0.359	16.79
		40 °C	13.87	0.329	0.9936	13.61	0.346	18.50
	Zn(II)	10 °C	6.27	0.356	0.9859	6.50	0.338	23.73
		20 °C	6.62	0.343	0.9876	6.82	0.328	23.04
		30 °C	7.07	0.326	0.9905	7.21	0.316	20.70
		40 °C	7.59	0.306	0.9913	7.66	0.301	19.17

3.2.7) Adsorption Thermodynamic

The thermodynamic parameters: Gibb's free energy change ($\Delta G°$), enthalpy change ($\Delta H°$), and entropy change ($\Delta S°$) were calculated by the method proposed by Khan and Singh [116]. They stated that the thermodynamic parameters can be calculated from the variation of thermodynamic equilibrium constant, K_d (or the thermodynamic distribution coefficient), with change in temperature. K_d for the adsorption reaction can be defined as

$$K_d = \frac{a_s}{a_e} = \frac{\nu_s C_s}{\nu_e C_e} \tag{3.17}$$

where a_s is the activity of the absorbed species (i.e., ions, molecules), a_e is the activity of the species in the equilibrium solution, C_s is the surface concentration of species in moles per gram of adsorbent and C_e is the concentration of species in equilibrium suspension, ν_s is the activity coefficient of the adsorbed species, and ν_e is the activity coefficient of the species in the equilibrium solution. As the concentration of the species in the solution approaches zero, the activity coefficient approaches unity. Equation (3.17) may then be written as:

$$\lim_{C_S \to 0} \frac{C_s}{C_e} = \frac{a_s}{a_e} = K_d \tag{3.18}$$

Values of K_d are obtained by plotting ln (C_s/C_e) versus C_s and extrapolating to zero C_s. C_s is the concentration of species at the surface which is similar to q_e. For convenience, q_e is used instead. The $\Delta G°$ was calculated from the Van't Hoff equation:

$$\Delta G° = -RT \ln K_d \tag{3.19}$$

where R is the gas constant (8.314 J/mol K), and T is the temperature (K).

The $\Delta H°$ and $\Delta S°$ were calculated from the slope and intercept, respectively, of the plot of ln K_d against $1/T$ of the Van't Hoff equation:

$$\ln K_d = \left(\frac{-\Delta H°}{R}\right)\frac{1}{T} + \frac{\Delta S°}{R} \tag{3.20}$$

The plots of ln (q_e/C_e) versus q_e of Cd(II) and Zn(II) at the temperature of 10 − 40 °C are illustrated in Figs. 3.25 and 3.26, respectively. The plots of ln K_d against 1/T of Cd(II) and Zn(II) at different temperature are shown in Figs. 3.27 and 3.28, respectively. The values of R^2 of ln q_e/C_e against q_e plots, ln K_d, and thermodynamic parameters are summarized in Table 3.10. It was found that the values of $\Delta G°$ were negative for all the temperatures for both metals. This confirmed that the adsorption of Cd(II) and Zn(II) on leonardite was spontaneous process. The $\Delta H°$ was 20.38 kJ/mol for Cd(II) and 17.88 kJ/mol for Zn(II). The positive values of $\Delta H°$ suggested the endothermic adsorption. The positive value of $\Delta S°$ indicated an increased in randomness at solid/liquid interface during adsorption.

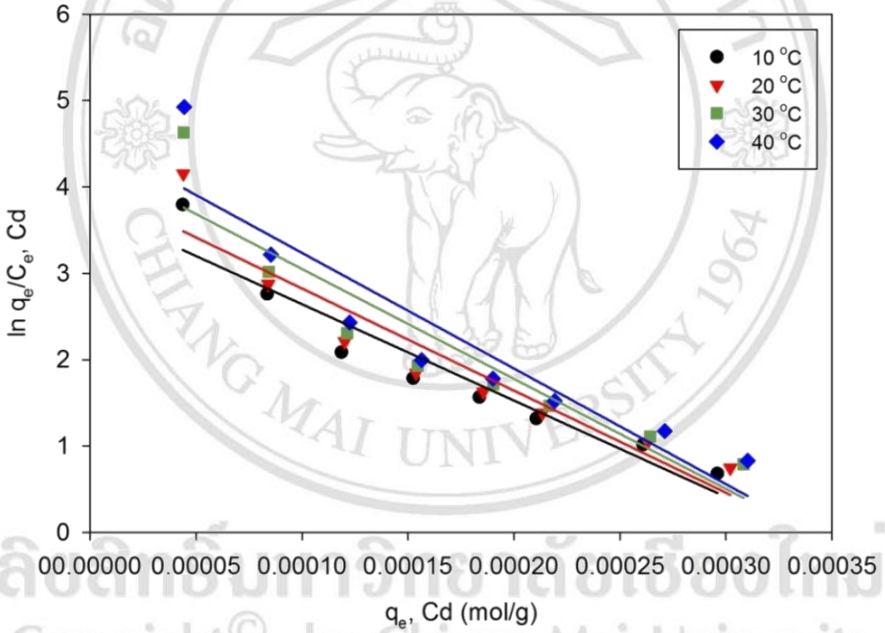

Fig. 3.25 Ln q_e/C_e against q_e of Cd(II) at 10, 20, 30, and 40 °C

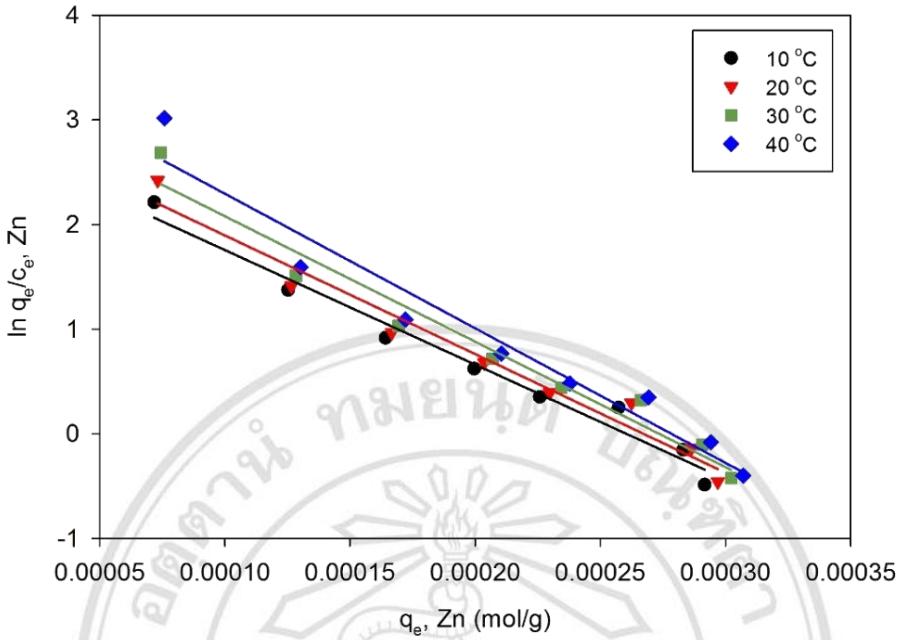

Fig. 3.26 Ln q_e/C_e against q_e of Zn(II) at 10, 20, 30, and 40 °C

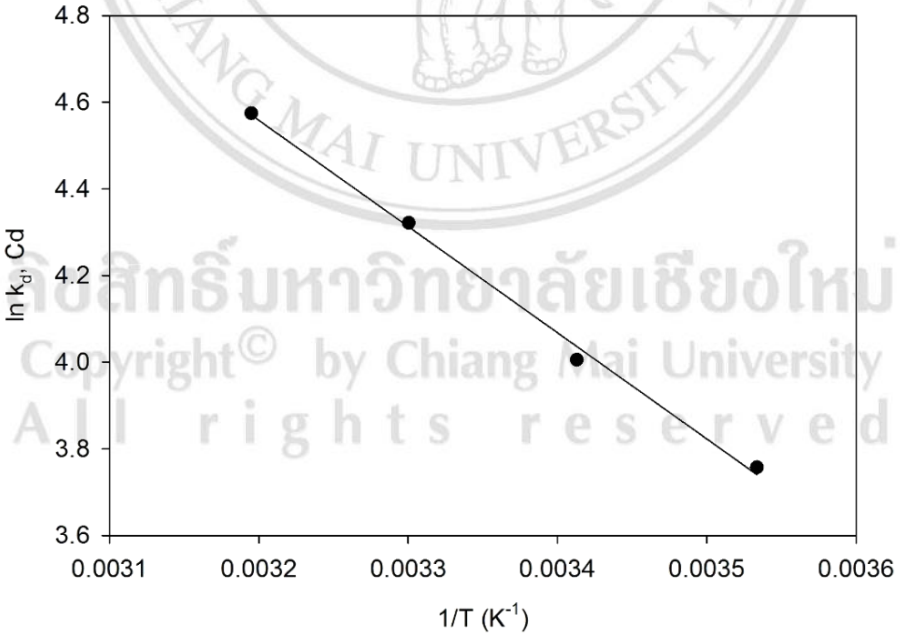

Fig. 3.27 Ln K_d against $1/T$ of Cd(II)

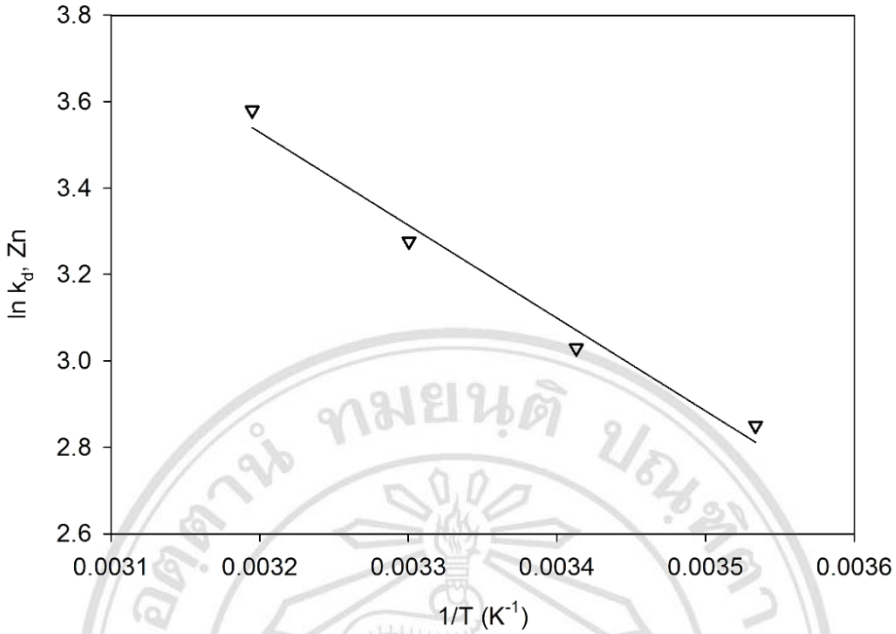

Fig. 3.28 Ln K_d against 1/T of Zn(II)

Table 3.10 Thermodynamic parameters of Cd(II) and Zn(II)

Metal ion	Temperature (°C)	R^2 (ln q_e/C_e vs. q_e)	ln K_d	$\Delta G°$ (kJ/mol)	$\Delta H°$ (kJ/mol)	$\Delta S°$ (J/mol.K)
Cd(II)	10	0.9176	3.76	-8.80	20.38	103.1
	20	0.8956	4.01	-9.83		
	30	0.8646	4.32	-10.86		
	40	0.8577	4.57	-11.89		
Zn(II)	10	0.9751	2.85	-6.62	17.88	86.55
	20	0.9670	3.03	-7.48		
	30	0.9606	3.28	-8.35		
	40	0.9475	3.58	-9.21		

3.3 Binary-components adsorption of Cd(II) and Zn(II) ions

In binary adsorption systems, the experiments were performed with the same conditions as single system. The mixture of leonardite and metal solution was adjusted to pH 6. The mixture was shaken for 60 min in water-bath shaker at 30 °C. The initial concentration of Cd(II) and Zn(II) in binary system were in the range of 5 – 30 mg/L. Various ratios of initial metal concentration were investigated. Adsorption isotherms of Cd(II) and Zn(II) in binary system are presented in Figs. 3.29 and 3.30, respectively.

Generally, the ionic interaction in multi-components system can be classified into 3 types by the ratio of the equilibrium adsorbed amount in multi-components system, q_{mix} and the equilibrium adsorbed amount in one-component system, q_0 [27].

Type I: $q_{mix}/q_0 > 1$, it indicates that the presence of the other metal ions in the adsorption system can increase the metal adsorbed amount (synergistic adsorption).

Type II: $q_{mix}/q_0 < 1$, the presence of the other metal ions decreases the metal adsorbed amount (antagonistic adsorption).

Type III: $q_{mix}/q_0 = 1$, the addition of other metal ions has no effect on the adsorption capacity.

From the results, it was found that the presence of Zn(II) in the Cd(II) adsorption systems resulted in the reducing of Cd(II) adsorbed amount. With the increase of Zn(II) concentration, adsorption uptake of Cd(II) tended to be much lower. For example, at Cd(II) initial concentration of 30 mg/L, Cd(II) adsorbed amount decreased from 24.4 to 10.9 mg/g. Since the q_{mix} was lower than q_0, thus q_{mix}/q_0 values were less than 1 for all ratios. Similarly, the adsorption of Zn(II) was suppressed by Cd(II). At Zn(II) initial concentration of 30 mg/L, adsorption capacity of Zn(II) reduced from 17.4 to 7.9 mg/g. Therefore, the adsorption of Cd(II) and Zn(II) in binary system was “antagonistic adsorption”. The competition between Cd(II) and Zn(II) for adsorption site led to the lower adsorption capacity.

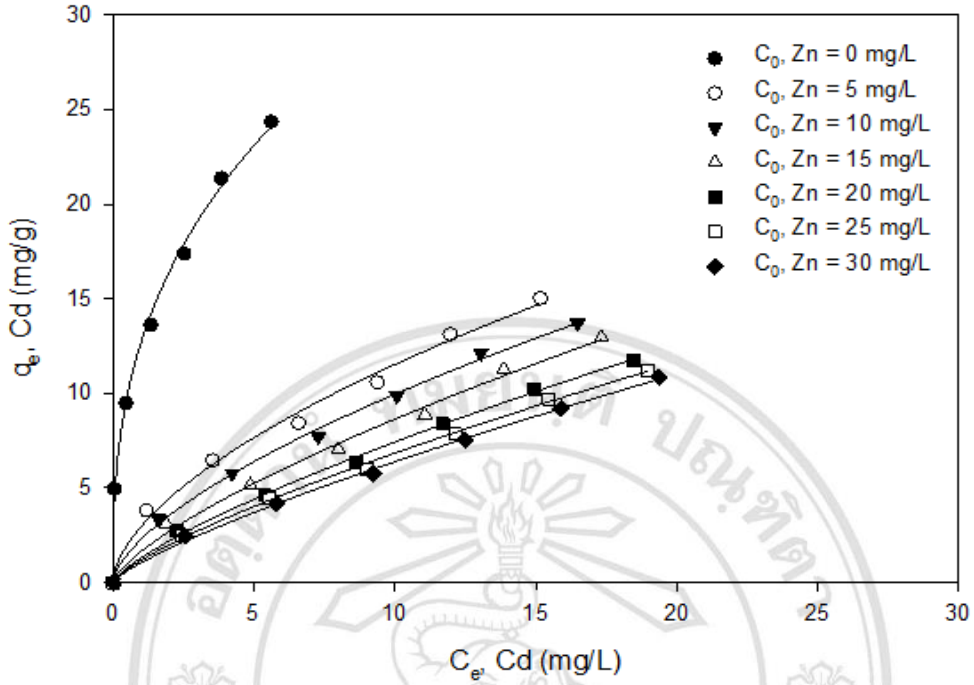

Fig. 3.29 Adsorption isotherm of Cd(II) in binary system

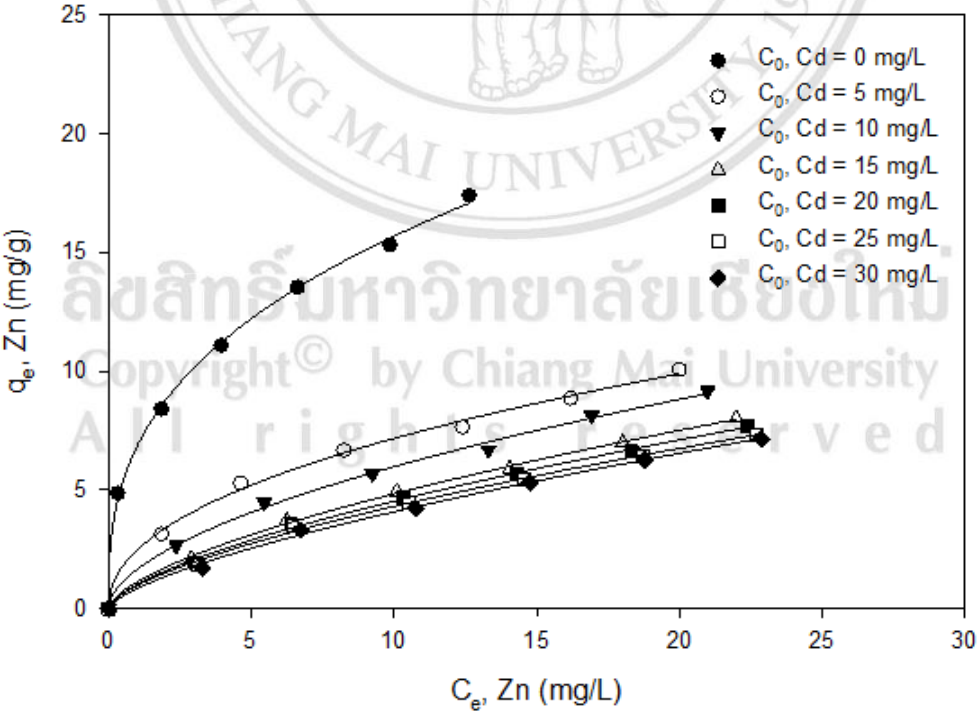

Fig. 3.30 Adsorption isotherm of Zn(II) in binary system

Table 3.11 Multi-components isotherm equations

Isotherm	Equation	Isotherm	Equation
Extended Langmuir	$q_{e,i} = \frac{q_{m,i} b_i C_{e,i}}{1 + \sum_{j=1}^{N} b_j C_{e,j}}$	SRS	$q_{e,i} = K_{F,i} C_{e,i} \left(\sum_{j=1}^{N} a_{ij} C_{e,j} \right)^{(1/n_i)-1}$
Modified Langmuir	$q_{e,i} = \frac{q_{m,i} b_i \left(C_{e,i} / \eta_i \right)}{1 + \sum_{j=1}^{N} b_j \left(C_{e,j} / \eta_j \right)}$	Extended Freundlich	$q_{e,i} = \frac{K_{F,i} C_{e,i}^{(1/n_i)+x_i}}{C_{e,i}^{x_i} + y_i C_{e,j}^{z_i}}$

Adsorption data of Cd(II) and Zn(II) in binary system were analyzed by 4 multi-components isotherms: Extended Langmuir, Modified Langmuir, Sheindorf-Rebuhn-Sheintuch (SRS) and Extended Freundlich isotherms. The isotherm equations are summarized in Table 3.11.

These isotherms used the information of single isotherm for predicting the adsorption in the multi-components system. The multi-components isotherm equations are more complex than single component isotherm equations. The application of linear regression technique for analysis of adsorption data is quite difficult. Therefore, only non-linear optimization method was employed. The applicable of these isotherms in representing the adsorption data was evaluated using 5 error functions (RMSE, ERRSQ, MAPE, MPSD and χ^2). The isotherm model which provides the lowest error value will be accepted to be the optimal isotherm model. Table 3.12 presents the isotherm parameters, error values and SNE values of isotherm models for the adsorption of Cd(II) and Zn(II) in binary systems.

Among the 4 multi-components adsorption isotherms, Extended Langmuir isotherm showed a poor fit to the adsorption data with the highest error values for all error functions. Considering the isotherm equation, Extended Langmuir isotherm equation does not include any parameter relating to the interaction between metal ions of different species. If there is any interaction between different species (synergistic or antagonistic adsorption), the prediction of Extended Langmuir will be less effective. Since Extended Langmuir equation does not compose of any parameter, the SNE value cannot be calculated.

Modified Langmuir isotherm provided the lower error values. It might be suggested that the Modified Langmuir interaction factor "η" can enhance the accuracy of Extended Langmuir isotherm. The interaction term "η" is the characteristic of each species and depends on the concentration of the other components [35]. The value of η_{Cd} was higher than η_{Zn}. The different values of η was determined from each error function except for RMSE and ERRSQ. The order of SNE value was RMSE ~ ERRSQ < MPSD < MAPE < χ^2. In this case, RMSE and ERRSQ provided the lowest SNE value. However, the best result was not obtained by using the Modified Langmuir isotherm model.

In the case of SRS isotherm, even though SRS isotherm is based on Freundlich isotherm and the adsorption data in the single system of both metal ions are more favored to Freundlich isotherm, the obtained error values were not satisfactory. The competition coefficients, a_{ij}, were determined from the binary adsorption data of Cd(II) and Zn(II). It describes the inhibition to the adsorption of component *i* by component *j*. The lower values of SRS parameter $a_{Cd\text{-}Zn}$ (4.62 − 5.68) than $a_{Zn\text{-}Cd}$ (5.53 − 7.00) indicated that the inhibition of Cd(II) adsorption by Zn(II) was less than the inhibition of Zn(II) adsorption by Cd(II). It confirmed the more favorably adsorbed of Cd(II). The order of SNE value was MPSD < χ^2 < RMSE ~ ERRSQ < MAPE. Parameter a_{ij} calculating by MPSD gave the smallest SNE value as compared to the other error functions.

Extended Freundlich isotherm showed a best fit to the adsorption data with the lowest error values from all error functions. This corresponds well to the equilibrium adsorption in the single system since the adsorptions of Cd(II) and Zn(II) in that system are more favored to Freundlich-type isotherm. Each of error function generated a set of Extended Freundlich isotherm parameter x_i, y_i and z_i. Like the single adsorption system, RMSE and ERRSQ provided the same isotherm parameter set and SNE value obtained from MPSD was the lowest when compared to other error functions. Thus, the parameter set produced from MPSD gave the acceptable fit to adsorption of Cd(II) and Zn(II) on leonardite in binary system. The relationship between experimental and calculated adsorbed amount of Cd(II) and Zn(II) for 4 multi-components isotherms are shown in Figs. 3.31(a)-(d).

The data points should lie on 45° line if the calculated and experimental adsorbed amount is similar. As seen, the deviation of data calculating by Extended Langmuir model

from the experimental data was large, especially Cd(II). For Modified Langmuir model, the prediction of adsorption data was quite good since the data points distributed around 45° line. For SRS model, it moderately estimated the adsorption data but there were some data points largely deviated from 45° line. Adsorbed amounts calculated from Extended Freundlich isotherm agreed well with experimental adsorbed amounts. Most data points lied on the line, only small number of deviated data was observed. Three-dimensional graphs representing the adsorption of Cd(II) and Zn(II) in binary system predicted by Extended Freundlich isotherm model were shown in Figs. 3.32 and 3.33, respectively. The surface graphs showed the prediction of isotherm model whereas the plots were experimental adsorption data. As can be seen, the predictions of Extended Freundlich isotherm model are found to be satisfactory.

Table 3.12 Adsorption isotherm parameters and error analysis for binary system

Adsorption isotherm	Parameter	Non-linear regression				
		RMSE	ERRSQ	MAPE	MPSD	χ^2
Extended Langmuir	error value	5.90	2504.8	69.60	227.18	160.17
Modified Langmuir	η_{Cd}	13.78	13.78	14.18	13.83	13.20
	η_{Zn}	7.08	7.08	7.22	7.03	6.71
	RMSE	**0.537**	0.537	0.543	0.538	0.552
	ERRSQ	20.77	**20.77**	21.26	20.86	21.96
	MAPE	7.319	7.319	**7.223**	7.339	7.728
	MPSD	23.91	23.91	24.02	**23.86**	24.35
	χ^2	4.640	4.640	4.865	4.624	**4.461**
	SNE	**4.801**	**4.801**	4.873	4.805	4.917
SRS	$a_{Cd\text{-}Zn}$	5.68	5.68	4.62	5.27	4.86
	$a_{Zn\text{-}Cd}$	7.00	7.00	5.53	6.36	5.79
	RMSE	**1.257**	1.257	1.481	1.289	1.394
	ERRSQ	113.70	**113.70**	157.86	119.70	139.87
	MAPE	17.57	17.57	**14.51**	15.92	14.77
	MPSD	48.98	48.98	51.13	**47.79**	49.18
	χ^2	18.24	18.24	14.79	15.47	**14.50**
	SNE	4.580	4.580	4.699	**4.372**	4.483

Table 3.12 Adsorption isotherm parameters and error analysis for binary system (Continued)

Adsorption isotherm	Parameter	Non-linear regression				
		RMSE	ERRSQ	MAPE	MPSD	χ^2
Extended Freundlich	x_{Cd}	0.553	0.553	0.509	0.518	0.511
	y_{Cd}	3.01	3.01	2.68	2.71	2.63
	z_{Cd}	0.437	0.437	0.452	0.449	0.452
	x_{Zn}	0.450	0.450	0.512	0.469	0.463
	y_{Zn}	2.45	2.45	2.77	2.48	2.43
	z_{Zn}	0.410	0.410	0.430	0.428	0.429
	RMSE	**0.308**	0.308	0.351	0.322	0.326
	ERRSQ	6.820	**6.820**	8.867	7.469	7.657
	MAPE	4.592	4.592	**4.209**	4.329	4.372
	MPSD	14.04	14.04	14.08	**13.44**	13.50
	χ^2	1.301	1.301	1.306	1.145	**1.133**
	SNE	4.639	4.639	4.917	**4.533**	4.571

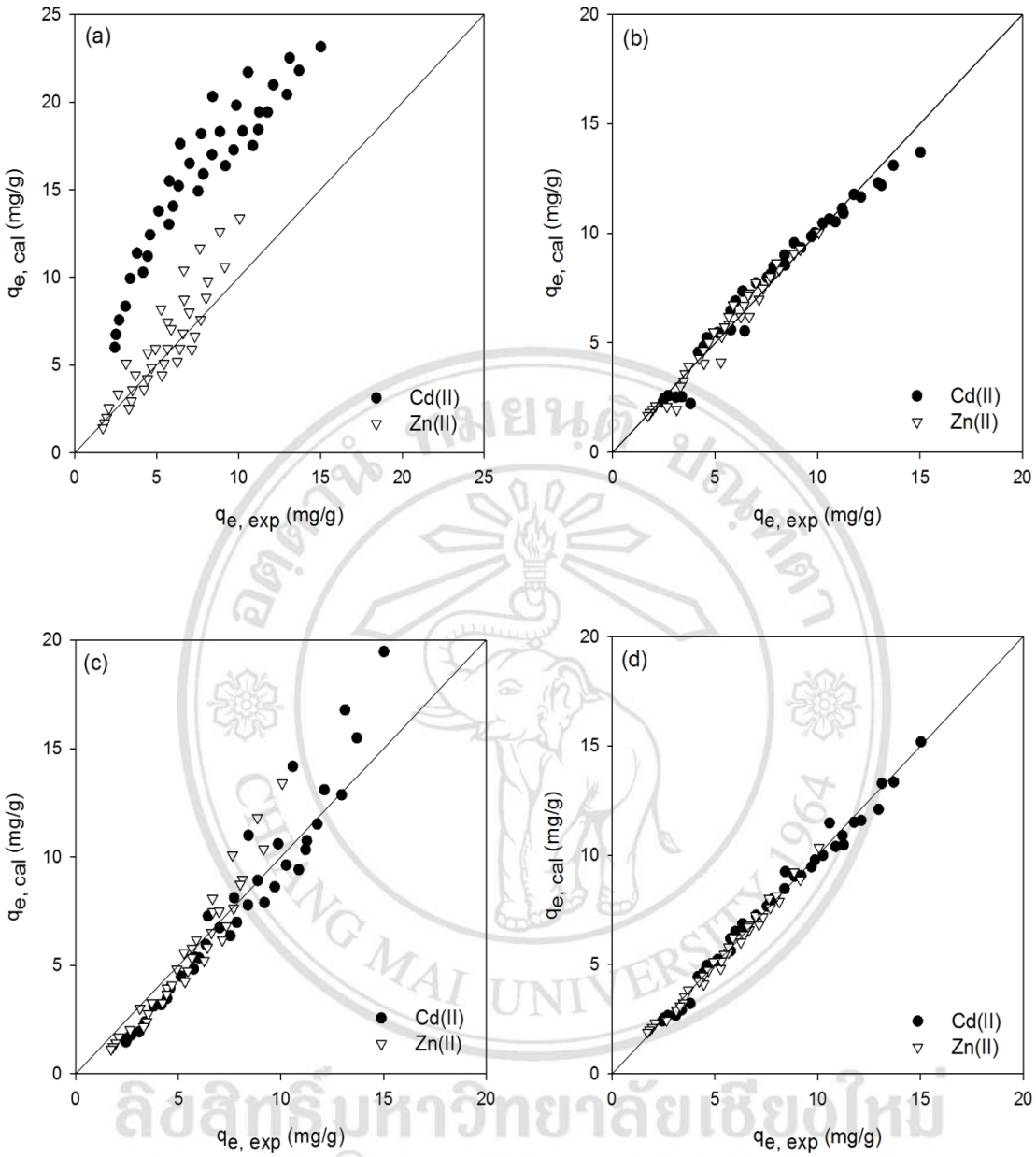

Figs. 3.31 The relationship between experimental and calculated adsorbed amount from multi-component isotherms for adsorption of Cd(II) and Zn(II) on leonardite

(a) Extended Langmuir isotherm (b) Modified Langmuir isotherm

(c) SRS isotherm (d) Extended Freundlich isotherm

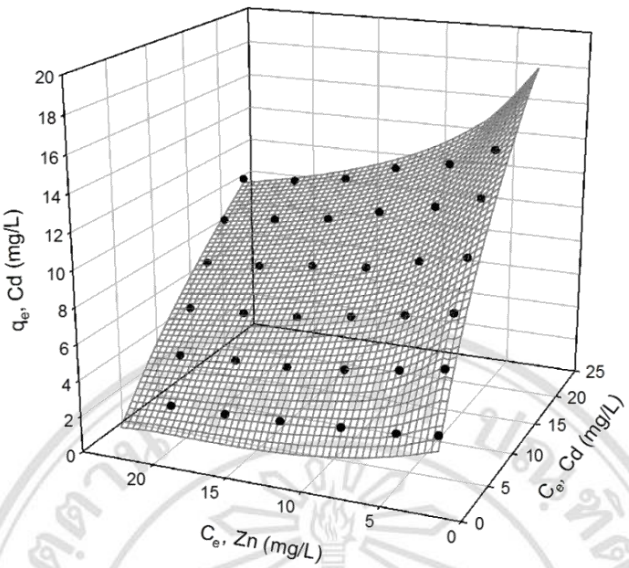

Fig. 3.32 Adsorption isotherm model of Cd(II) in binary system predicted by Extended Freundlich isotherm

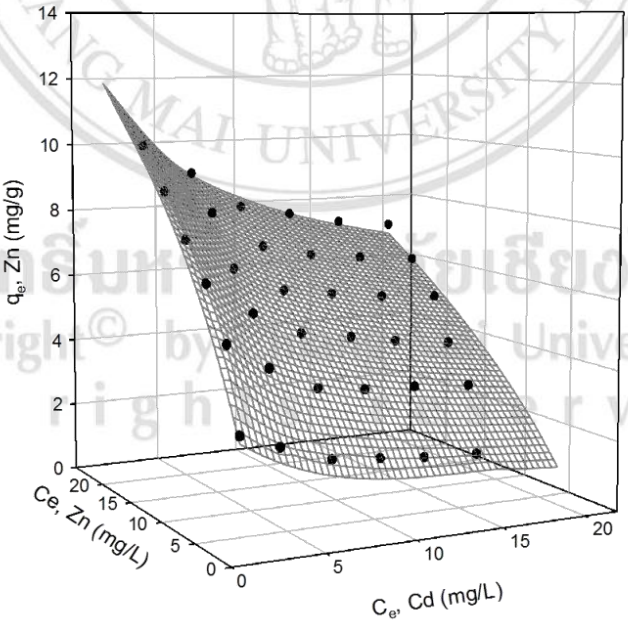

Fig. 3.33 Adsorption isotherm model of Zn(II) in binary system predicted by Extended Freundlich isotherm